

Online Statistical Inference of Constrained Stochastic Optimization via Random Scaling

Xinchen Du¹, Wanrong Zhu², Wei Biao Wu¹, and Sen Na³

¹Department of Statistics, The University of Chicago

²Department of Statistics, University of California, Irvine

³School of Industrial and Systems Engineering, Georgia Institute of Technology

Abstract

Constrained stochastic nonlinear optimization problems have attracted significant attention for their ability to model complex real-world scenarios in physics, economics, and biology. As datasets continue to grow, online inference methods have become crucial for enabling real-time decision-making without the need to store historical data. In this work, we develop an online inference procedure for constrained stochastic optimization by leveraging a method called Adaptive Inexact Stochastic Sequential Quadratic Programming (AI-SSQP). As a generalization of (sketched) Newton methods to constrained problems, AI-SSQP approximates the objective with a quadratic model and the constraints with a linear model at each step, then applies a randomized sketching solver to inexactly solve the resulting subproblem, along with an adaptive random stepsize to update the primal-dual iterates. Building on this design, we first establish the asymptotic normality guarantee of *averaged* AI-SSQP and observe that the averaged iterates exhibit better statistical efficiency than the last iterates, in terms of a smaller limiting covariance matrix. Furthermore, instead of estimating the limiting covariance matrix directly, we study a new online inference procedure called *random scaling*. Specifically, we construct a test statistic by appropriately rescaling the averaged iterates, such that the limiting distribution of the test statistic is free of any unknown parameters. Compared to existing online inference procedures, our approach offers two key advantages: (i) it enables the construction of *asymptotically valid* and *statistically efficient* confidence intervals, while existing procedures based on the last iterates are less efficient and rely on a plug-in covariance estimator that is inconsistent; and (ii) it is *matrix-free*, i.e., the computation involves only primal-dual iterates themselves without any matrix inversions, making its computational cost match that of advanced first-order methods for unconstrained problems. We validate our theoretical findings through numerical experiments on nonlinearly constrained regression problems and demonstrate the superior performance of random scaling over existing inference procedures.

1 Introduction

We consider the following constrained stochastic optimization problem:

$$\min_{\mathbf{x} \in \mathbb{R}^d} f(\mathbf{x}) = \mathbb{E}_{\xi \sim \mathcal{P}}[F(\mathbf{x}; \xi)], \quad \text{s.t. } c(\mathbf{x}) = \mathbf{0}, \quad (1)$$

where $f : \mathbb{R}^d \rightarrow \mathbb{R}$ is the objective function, $F(\mathbf{x}, \xi)$ is a noisy measurement of $f(\mathbf{x})$ with randomness ξ following distribution \mathcal{P} , and $c : \mathbb{R}^d \rightarrow \mathbb{R}^m$ denotes the equality constraints. Problem (1) arises in

various applications across science, economics, and engineering, such as portfolio allocation (Fan et al., 2012; Du et al., 2022), computer vision (Roy et al., 2018), PDE-constrained optimization (Rees et al., 2010; Kouri et al., 2014), constrained deep neural networks (Chen et al., 2018), physics-inspired neural networks (Cuomo et al., 2022), natural language processing (Nandwani et al., 2019), and constrained maximum likelihood estimation (Geyer, 1991; Chatterjee et al., 2016). In practice, Problem (1) can be interpreted as a constrained model parameter estimation problem, where ξ denotes the data sample, $f(\mathbf{x})$ denotes the expected loss, and the (primal) solution $\mathbf{x}^* = \operatorname{argmin}_{c(\mathbf{x})=\mathbf{0}} f(\mathbf{x})$ denotes the true model parameter. Let $\mathcal{L}(\mathbf{x}, \boldsymbol{\lambda}) = f(\mathbf{x}) + \boldsymbol{\lambda}^\top c(\mathbf{x})$ be the Lagrangian function, where $\boldsymbol{\lambda} \in \mathbb{R}^m$ is the dual vector associated with equality constraints; and let $\boldsymbol{\lambda}^*$ denote the dual solution. In this paper, our goal is to conduct online statistical inference for the primal-dual solution $(\mathbf{x}^*, \boldsymbol{\lambda}^*)$.

Using the classic offline method via sample average approximation (SAA), one can find the solution to the following problem:

$$\min_{\mathbf{x} \in \mathbb{R}^d} \hat{f}_t(\mathbf{x}) = \frac{1}{t} \sum_{i=1}^t F(\mathbf{x}; \xi_i), \quad \text{s.t. } c(\mathbf{x}) = \mathbf{0}, \quad (2)$$

where $\xi_1, \xi_2, \dots, \xi_t$ are observed i.i.d data from \mathcal{P} . It is well known that the minimizer $(\hat{\mathbf{x}}_t, \hat{\boldsymbol{\lambda}}_t)$ of (2), also called *constrained M-estimator*, exhibits \sqrt{t} -consistency and asymptotic normality, allowing us to perform statistical inference. In particular, under proper regularity conditions, we have that as $t \rightarrow \infty$ (Shapiro et al., 2014, Chapter 5),

$$\sqrt{t} \cdot (\hat{\mathbf{x}}_t - \mathbf{x}^*, \hat{\boldsymbol{\lambda}}_t - \boldsymbol{\lambda}^*) \xrightarrow{d} \mathcal{N}(\mathbf{0}, \boldsymbol{\Xi}^*), \quad (3)$$

where the limiting covariance is given by $\boldsymbol{\Xi}^* = (\nabla^2 \mathcal{L}(\mathbf{x}^*, \boldsymbol{\lambda}^*))^{-1} \operatorname{cov}(\nabla \mathcal{L}(\mathbf{x}^*, \boldsymbol{\lambda}^*; \xi)) (\nabla^2 \mathcal{L}(\mathbf{x}^*, \boldsymbol{\lambda}^*))^{-1}$ (see Section 3.2 for details). However, offline methods often have to deal with large batches of samples, leading to significant computational and memory cost. In recent years, a growing body of literature has focused on developing and analyzing *online* methods for solving the above constrained stochastic optimization problems and performing the underlying inference tasks. One simple online method is projection-based Stochastic Gradient Descent (SGD). Davis et al. (2019) proved almost-sure convergence for projection-based SGD, while Duchi and Ruan (2021) and Davis et al. (2024) established asymptotic normality guarantees for its iterates. However, the projection operator, which plays a key role in these methods, can be computationally expensive in practice, especially for nonlinear equality constraints in (1). To circumvent this difficulty, researchers have developed alternative constrained optimization methods, including penalty methods, barrier methods, augmented Lagrangian methods, and sequential quadratic programming methods (Bertsekas, 1997, 2014; Nocedal and Wright, 2006).

More recently, various stochastic sequential quadratic programming (SSQP) methods, which generalize stochastic Newton methods for unconstrained problems, have been proposed to efficiently solve constrained problems in an online fashion; see Berahas et al. (2021, 2024); Na et al. (2022, 2023); Fang et al. (2024); Curtis et al. (2024) and references therein. For the purpose of statistical inference, Na and Mahoney (2025) considered an Adaptive Inexact SSQP (AI-SSQP) scheme, where at each step the method employs an iterative sketching solver to inexactly solve the SQP quadratic subproblem and selects a suitable random stepsize (inspired by stochastic line search) to update the primal-dual iterate $(\mathbf{x}_t, \boldsymbol{\lambda}_t)$. The authors demonstrated that AI-SSQP iterates exhibit the following asymptotic normality property (see Section 3.2 for details) (Na and Mahoney, 2025, Theorem 5.6):

$$\sqrt{1/\bar{\alpha}_t} \cdot (\mathbf{x}_t - \mathbf{x}^*, \boldsymbol{\lambda}_t - \boldsymbol{\lambda}^*) \xrightarrow{d} \mathcal{N}(0, \tilde{\boldsymbol{\Xi}}^*), \quad (4)$$

where $\bar{\alpha}_t$ is the random stepsize and the limiting covariance $\tilde{\Xi}^*$ (given by (19)) is determined by the underlying sketching distribution. AI-SSQP methods offer advantages over projection-based methods by linearizing nonlinear constraints, thereby eliminating the need for costly projection operators. Additionally, the sketching solver introduces a trade-off between computational and statistical efficiency. In particular, when the sketching solver is suppressed and the quadratic subproblem is solved exactly, the AI-SSQP iterates achieve primal-dual *asymptotic minimax efficiency*, with the limiting covariance $\tilde{\Xi}^*$ reducing to the optimal covariance Ξ^* achieved by the constrained M -estimator $(\hat{\mathbf{x}}_t, \hat{\boldsymbol{\lambda}}_t)$ in (3). The primal component of this covariance also matches that obtained by projection-based methods in [Duchi and Ruan \(2021\)](#); [Davis et al. \(2024\)](#).

To facilitate online inference via asymptotic normality, a suitable covariance matrix estimator is typically required. [Jiang et al. \(2025\)](#) analyzed a *batch-means* covariance estimator originally developed for SGD methods ([Chen et al., 2020](#); [Zhu et al., 2021](#)), and demonstrated that the same estimator applies to projected SGD methods with the same convergence rate. However, due to the nonlinearity and nonconvexity of the problem, the convergence analysis of the batch-means estimator was conducted only under light-tailed gradient noise, a stronger condition than that required for asymptotic normality of projected SGD. [Kuang et al. \(2025\)](#) designed a *batch-free* covariance estimator for stochastic Newton methods and established an improved convergence rate under strong convexity. Their analysis also does not apply to nonlinear problem (1). In fact, [Na and Mahoney \(2025\)](#) introduced a *plug-in* covariance estimator for $\tilde{\Xi}^*$ in (4) within the AI-SSQP framework. However, due to the difficulty of estimating the sketching components of $\tilde{\Xi}^*$, their estimator neglects all such components and instead estimates Ξ^* . This leads to two main limitations. First, the resulting covariance estimator is generally inconsistent due to the approximation error incurred by the sketching solver ([Na and Mahoney, 2025](#), Theorem 5.10). It is consistent only when the sketching solver is suppressed; and the bias significantly undermines the validity of statistical inference. Second, the method requires inverting the estimated Hessian matrix, which incurs a computational cost of $O((d+m)^3)$. This cost often exceeds that of solving the Newton subproblems themselves, contradicting the spirit of utilizing sketching solvers.

To overcome the above challenges, we leverage a technique called *random scaling* to bypass the need for direct covariance matrix estimation. Specifically, instead of focusing on the asymptotic normality of the *last* iterate of AI-SSQP, we consider the averaged iterate $(\bar{\mathbf{x}}_t, \bar{\boldsymbol{\lambda}}_t) := \frac{1}{t} \sum_{i=0}^{t-1} (\mathbf{x}_i, \boldsymbol{\lambda}_i)$ and establish its asymptotic normality:

$$\sqrt{t} \cdot (\bar{\mathbf{x}}_t - \mathbf{x}^*, \bar{\boldsymbol{\lambda}}_t - \boldsymbol{\lambda}^*) \xrightarrow{d} \mathcal{N}(0, \bar{\Xi}^*),$$

where the limiting covariance matrix $\bar{\Xi}^*$ differs from $\tilde{\Xi}^*$ of the last iterate in (4). Similar to $\tilde{\Xi}^*$, when the sketching solver is degraded, $\bar{\Xi}^*$ reduces to the minimax optimal covariance Ξ^* . However, when the sketching solver is deployed, we show that the averaged iterate enjoys better statistical efficiency with $\bar{\Xi}^* \preceq \tilde{\Xi}^*$. Furthermore, to perform statistical inference, instead of estimating $\bar{\Xi}^*$, we exploit a *random scaling* matrix that can be updated on-the-fly:

$$V_t = \frac{1}{t^2} \sum_{i=1}^t i^2 \begin{pmatrix} \mathbf{x}_i - \bar{\mathbf{x}}_t \\ \boldsymbol{\lambda}_i - \bar{\boldsymbol{\lambda}}_t \end{pmatrix} \begin{pmatrix} \mathbf{x}_i - \bar{\mathbf{x}}_t \\ \boldsymbol{\lambda}_i - \bar{\boldsymbol{\lambda}}_t \end{pmatrix}^\top,$$

and studentize $(\bar{\mathbf{x}}_t, \bar{\boldsymbol{\lambda}}_t)$ using V_t . In particular, we prove that the resulting test statistic is *asymptotically pivotal*: for any $\mathbf{w} \in \mathbb{R}^{d+m}$,

$$\frac{\sqrt{t} \cdot \mathbf{w}^\top (\bar{\mathbf{x}}_t - \mathbf{x}^*, \bar{\boldsymbol{\lambda}}_t - \boldsymbol{\lambda}^*)}{\sqrt{\mathbf{w}^\top V_t \mathbf{w}}} \xrightarrow{d} \frac{W_1(1)}{\sqrt{\int_0^1 (W_1(r) - rW_1(1))^2 dr}}$$

where $W_1(\cdot)$ denotes the standard one-dimensional Brownian motion. Our pivotal test statistic offers four key advantages.

- (i) Since both the averaged iterate $(\bar{\mathbf{x}}_t, \bar{\boldsymbol{\lambda}}_t)$ and the random scaling matrix V_t can be updated recursively, our inference method is well-suited for online computation.
- (ii) Our method enables the construction of asymptotically valid confidence intervals for the true parameters $(\mathbf{x}^*, \boldsymbol{\lambda}^*)$, resolving the inconsistency of the plug-in estimator in [Na and Mahoney \(2025\)](#).
- (iii) Our test statistic based on second-order methods is matrix-free (i.e., no matrix inversion). Therefore, the memory and computational complexities of our inference procedure leveraging second-order methods match those of first-order methods, i.e., $O((d + m)^2)$.
- (iv) Our inference method is applicable to a broad class of constrained nonlinear problems. In contrast, existing inference literature based on SGD or stochastic Newton methods focuses on unconstrained strongly convex problems ([Chen et al., 2020](#); [Zhu et al., 2021](#); [Wei et al., 2023](#); [Chen et al., 2024](#); [Kuang et al., 2025](#)) (a detailed literature review is deferred later), while projection-based methods such as [Davis et al. \(2024\)](#); [Jiang et al. \(2025\)](#) rely on sub-Gaussian gradient noise assumptions.

We demonstrate the promising empirical performance of our random scaling method through nonlinearly constrained regression problems.

Related work on unconstrained online inference. We present a brief overview of the unconstrained online statistical inference problem, which serves as the foundation for our study of the constrained inference problem.

Early works established almost-sure convergence of SGD under various assumptions ([Robbins and Monro, 1951](#); [Kiefer and Wolfowitz, 1952](#); [Robbins and Siegmund, 1971](#)). Later, [Polyak and Juditsky \(1992\)](#) proved the asymptotic normality of averaged SGD iterates, with the limiting covariance matrix given by $\Sigma^* = (\nabla^2 f(\mathbf{x}^*))^{-1} \text{cov}(\nabla F(\mathbf{x}^*; \xi))(\nabla^2 f(\mathbf{x}^*))^{-1}$. Since Σ^* is generally unknown, recent work by [Fang et al. \(2018\)](#) developed a bootstrap procedure to construct confidence intervals by approximating the limiting distribution using empirical bootstrap samples. To avoid high computational cost of bootstrap, later studies focused on covariance matrix estimation. [Chen et al. \(2020\)](#) designed an online plug-in estimator for Σ^* by separately estimating $(\nabla^2 f(\mathbf{x}^*))^{-1}$ and $\text{cov}(\nabla F(\mathbf{x}^*; \xi))$ using sample averages. Although this estimator performs well, it requires computing the Hessian inverse, which is intrusive and unnecessary for SGD updates themselves. As an alternative, [Zhu et al. \(2021\)](#) proposed an online batch-means covariance estimator using only SGD iterates. While this approach is more computationally efficient, it suffers from a slow convergence rate. In practice, estimating the full covariance matrix can be difficult and is often unnecessary, especially when the primary goal is to construct confidence intervals. Consequently, recent work has focused on developing asymptotically pivotal statistics for online inference in SGD, thereby avoiding the need for accurate covariance matrix estimation. One such approach is the random scaling method ([Lee et al., 2022](#)), which self-normalizes the estimation error of averaged SGD iterates using a random scaling matrix. This technique has demonstrated promising performance across a wide range of optimization algorithms, including ROOT-SGD ([Luo et al., 2022](#)), stochastic approximation under Markovian data ([Li et al., 2023](#)), weighted-averaged SGD ([Wei et al., 2023](#)), and the Kiefer–Wolfowitz algorithm ([Chen et al., 2024](#)). We extend the above literature by applying random scaling technique to AI-SSQP methods for constrained inference problems.

Another line of related literature focuses on online inference using second-order methods. [Leluc and Portier \(2023\)](#) established asymptotic normality for the last iterate of conditioned SGD and observed that the limiting covariance achieves optimality when the conditioning matrix is the Hessian.

Bercu et al. (2020) designed an online Newton method for logistic regression, and Boyer and Godichon-Baggioni (2023); Cénac et al. (2025) extended that approach to more general regression problems. Although the aforementioned works provided asymptotic normality guarantees comparable to those for first-order methods, they do not offer a clear approach for performing online inference based on the normality property. Moreover, these methods are restricted to regression and/or convex problems, making them inapplicable to the nonlinear problems considered in our work. For example, the Hessian inverse in regression problems often exhibits a nice structure as a sum of rank-one matrices, enabling efficient Hessian inverse updates via the Sherman–Morrison formula. However, this computational advantage, relying on specific problem structures, does not extend to constrained regression problems. To our knowledge, this paper presents the first asymptotically valid inference procedure for nonlinear and nonconvex problems using second-order methods, with a computational cost matching that of state-of-the-art first-order methods.

1.1 Organization and notation

We begin by reviewing the AI-SSQP method in Section 2. Section 3 presents the assumptions and establishes the asymptotic normality of the averaged AI-SSQP iterates. In Section 4, we introduce the pivotal test statistic and develop its theoretical properties. Numerical experiments and conclusions are provided in Sections 5 and 6, respectively. All proofs are deferred to the appendices.

We let $\|\cdot\|$ denote the ℓ_2 norm for vectors and spectral norm for matrices, $\|\cdot\|_F$ denote the Frobenius norm for matrices, and $\text{Tr}(\cdot)$ denote the trace of a matrix. For two sequences $\{a_t, b_t\}$, $a_t = O(b_t)$ (also written as $a_t \lesssim b_t$) implies that $|a_t| \leq c|b_t|$ for sufficient large t , where c is a positive constant. Similarly, $a_t = o(b_t)$ implies that $|a_t/b_t| \rightarrow 0$ as $t \rightarrow \infty$. We let I denote the identity matrix, $\mathbf{0}$ denote the zero vector or matrix, and \mathbf{e}_i denote the vector with 1 at the i -th entry and 0 elsewhere. We let $\mathbf{1}_{\{\cdot\}}$ denote the indicator function and $\lfloor \cdot \rfloor$ denote the floor function, which rounds down to the nearest integer. For a sequence of compatible matrices $\{A_i\}_i$, $\prod_{k=i}^j A_k = A_j A_{j-1} \cdots A_i$ when $j \geq i$ and I when $j < i$. For two matrices A and B , $A \succeq B$ means that $A - B$ is positive semidefinite. We reserve the notation $G(\mathbf{x})$ to denote the constraints Jacobian, that is, $G(\mathbf{x}) = \nabla c(\mathbf{x}) = (\nabla c_1(\mathbf{x}), \dots, \nabla c_m(\mathbf{x}))^\top \in \mathbb{R}^{m \times d}$. Let $\mathcal{L}(\mathbf{x}, \boldsymbol{\lambda}) = f(\mathbf{x}) + \boldsymbol{\lambda}^\top c(\mathbf{x})$ denote the Lagrangian function of (1), where $\boldsymbol{\lambda} \in \mathbb{R}^m$ is the dual vector associated with equality constraints. For simplicity, we let $f_t = f(\mathbf{x}_t)$, $c_t = c(\mathbf{x}_t)$, $\nabla \mathcal{L}_t = \nabla \mathcal{L}(\mathbf{x}_t, \boldsymbol{\lambda}_t)$ (similar for ∇f_t , G_t etc.); and $f^* = f(\mathbf{x}^*)$, $c^* = c(\mathbf{x}^*)$, $\nabla \mathcal{L}^* = \nabla \mathcal{L}(\mathbf{x}^*, \boldsymbol{\lambda}^*)$ (similar for ∇f^* , G^* etc.). The bar notation $(\bar{\cdot})$ denotes random quantities at each step, except for the averaged iterate $(\bar{\mathbf{x}}_t, \bar{\boldsymbol{\lambda}}_t) = \sum_{i=0}^{t-1} (\mathbf{x}_i, \boldsymbol{\lambda}_i)/t$. For example, $\bar{\nabla}_{\mathbf{x}} \mathcal{L}_t$ is the random estimate of $\nabla_{\mathbf{x}} \mathcal{L}$ at the step t .

2 Adaptive Inexact Stochastic Sequential Quadratic Programming

In this section, we review the AI-SSQP method for solving Problem (1). For constrained problems, it is known that under certain constraint qualifications (cf. Assumption 3.1), the first-order necessary condition for $(\mathbf{x}^*, \boldsymbol{\lambda}^*)$ to be a local solution of (1) is the KKT condition $\nabla \mathcal{L}^* = \nabla \mathcal{L}(\mathbf{x}^*, \boldsymbol{\lambda}^*) = \mathbf{0}$ (Nocedal and Wright, 2006). As such, AI-SSQP applies Newton’s method to the equation $\nabla \mathcal{L}(\mathbf{x}, \boldsymbol{\lambda}) = \mathbf{0}$ in three steps: estimating the objective gradient and Hessian, (inexactly) solving Newton’s system, and updating the primal-dual iterate. We refer to Na and Mahoney (2025) for further details.

- **Step 1: Estimate objective gradient and Hessian.** Given the current iterate $(\mathbf{x}_t, \boldsymbol{\lambda}_t)$, we

draw a sample $\xi_t \sim \mathcal{P}$ and compute the stochastic objective gradient and Hessian estimates as

$$\bar{g}_t = \nabla F(\mathbf{x}_t; \xi_t) \quad \text{and} \quad \bar{H}_t = \nabla^2 F(\mathbf{x}_t; \xi_t).$$

Recalling the Jacobian matrix of the constraints $G_t = \nabla c_t$, we then compute the stochastic estimates of the Lagrangian gradient and Hessian with respect to \mathbf{x} as

$$\bar{\nabla}_{\mathbf{x}} \mathcal{L}_t = \bar{g}_t + G_t^\top \boldsymbol{\lambda}_t \quad \text{and} \quad \bar{\nabla}_{\mathbf{x}}^2 \mathcal{L}_t = \bar{H}_t + \sum_{j=1}^m [\boldsymbol{\lambda}_t]_j \nabla^2 c_j(\mathbf{x}_t).$$

Next, we define the regularized averaged Hessian B_t :

$$B_t = \frac{1}{t} \sum_{i=0}^{t-1} \bar{\nabla}_{\mathbf{x}}^2 \mathcal{L}_i + \Delta_t,$$

where $\Delta_t = \Delta(\mathbf{x}_t, \boldsymbol{\lambda}_t)$ is a Hessian regularization term chosen such that B_t is positive definite in the null space $\{\mathbf{x} \in \mathbb{R}^d : G_t \mathbf{x} = \mathbf{0}\}$. This regularization, combined with the constraint qualification condition (LICQ, cf. Assumption 3.1), ensures that the SQP subproblem (5) admits a unique solution. For convex problems, we may simply set $\Delta_t = \mathbf{0}$ for all t ; for general constrained problems, we may choose $\Delta_t = \delta_t I$ for a large enough $\delta_t > 0$ (Nocedal and Wright, 2006). In addition, we highlight that B_t is an average over the samples $\{\xi_i\}_{i=0}^{t-1}$, suggesting that B_t and Δ_t are deterministic given $(\mathbf{x}_t, \boldsymbol{\lambda}_t)$. The averaging facilitates the convergence of the Hessian matrix (i.e., the law of large numbers for martingales), while excluding ξ_t reduces the conditional bias of the stochastic Newton direction (see (6)).

• **Step 2: Inexactly solve the SQP subproblem.** With the quantities $\bar{g}_t, G_t, \bar{\nabla}_{\mathbf{x}} \mathcal{L}_t, B_t$, we then formulate the SQP subproblem by performing a quadratic approximation to the objective and a linear approximation to the constraints. Specifically, we aim to solve the following quadratic program:

$$\min_{\tilde{\Delta} \mathbf{x}_t} \frac{1}{2} \tilde{\Delta} \mathbf{x}_t^\top B_t \tilde{\Delta} \mathbf{x}_t + \bar{g}_t^\top \tilde{\Delta} \mathbf{x}_t, \quad \text{s.t.} \quad c_t + G_t \tilde{\Delta} \mathbf{x}_t = \mathbf{0}. \quad (5)$$

It can be shown that the above quadratic program is equivalent to the linear system

$$\underbrace{\begin{pmatrix} B_t & G_t^\top \\ G_t & \mathbf{0} \end{pmatrix}}_{K_t} \underbrace{\begin{pmatrix} \tilde{\Delta} \mathbf{x}_t \\ \tilde{\Delta} \boldsymbol{\lambda}_t \end{pmatrix}}_{\tilde{\mathbf{z}}_t} = - \underbrace{\begin{pmatrix} \bar{\nabla}_{\mathbf{x}} \mathcal{L}_t \\ c_t \end{pmatrix}}_{\bar{\nabla} \mathcal{L}_t}. \quad (6)$$

Solving the above Newton system by computing K_t^{-1} to derive the exact stochastic Newton direction $\tilde{\mathbf{z}}_t := (\tilde{\Delta} \mathbf{x}_t, \tilde{\Delta} \boldsymbol{\lambda}_t)$ incurs a computational complexity of $O((d+m)^3)$, which is less competitive compared to first-order methods. To reduce the computational overhead, we employ a sketching solver to derive an approximate solution.

In particular, for each t , we perform τ sketching steps. At each sketching step j , we independently generate a random sketching matrix/vector $S_{t,j} \in \mathbb{R}^{(d+m) \times q}$ for some $q \geq 1$ from a distribution S , and aim to solve the following sketched Newton system:

$$S_{t,j}^\top K_t \mathbf{z} = -S_{t,j}^\top \bar{\nabla} \mathcal{L}_t.$$

However, this sketched system generally has multiple solutions, including the exact Newton direction $\tilde{\mathbf{z}}_t$. We prefer the solution that is closest to the current solution approximation $\mathbf{z}_{t,j}$, that is ($\mathbf{z}_{t,0} = \mathbf{0}$),

$$\mathbf{z}_{t,j+1} = \arg \min_{\mathbf{z}} \|\mathbf{z} - \mathbf{z}_{t,j}\|^2 \quad \text{s.t.} \quad S_{t,j}^\top K_t \mathbf{z} = -S_{t,j}^\top \bar{\nabla} \mathcal{L}_t. \quad (7)$$

The closed form solution to (7) is given by:

$$\mathbf{z}_{t,j+1} = \mathbf{z}_{t,j} - K_t S_{t,j} (S_{t,j}^\top K_t^2 S_{t,j})^\dagger S_{t,j}^\top (K_t \mathbf{z}_{t,j} + \bar{\nabla} \mathcal{L}_t), \quad 0 \leq j \leq \tau - 1, \quad (8)$$

where $(\cdot)^\dagger$ denotes the Moore–Penrose pseudoinverse. Finally, we define

$$(\bar{\Delta} \mathbf{x}_t, \bar{\Delta} \boldsymbol{\lambda}_t) := \mathbf{z}_{t,\tau} \quad (9)$$

as our approximate Newton direction.

• **Step 3: Adaptive stepsize.** With the approximate Newton direction $(\bar{\Delta} \mathbf{x}_t, \bar{\Delta} \boldsymbol{\lambda}_t) = \mathbf{z}_{t,\tau}$, we finally update the iterate $(\mathbf{x}_t, \boldsymbol{\lambda}_t)$ with an adaptive random stepsize $\bar{\alpha}_t$:

$$(\mathbf{x}_{t+1}, \boldsymbol{\lambda}_{t+1}) = (\mathbf{x}_t, \boldsymbol{\lambda}_t) + \bar{\alpha}_t \cdot (\bar{\Delta} \mathbf{x}_t, \bar{\Delta} \boldsymbol{\lambda}_t). \quad (10)$$

The AI-SSQP method allows any adaptive stepsize selection scheme as long as the safeguard condition holds:

$$0 < \beta_t \leq \bar{\alpha}_t \leq \eta_t \quad \text{with} \quad \eta_t = \beta_t + \chi_t. \quad (11)$$

Here, $\{\beta_t, \eta_t\}$ are sequences serving as lower and upper bounds, respectively, and χ_t represents the adaptivity gap between them. See [Berahas et al. \(2021, 2024\)](#); [Curtis et al. \(2024\)](#); [Na and Mahoney \(2025\)](#) for line-search-based stepsize selection schemes that adhere to the safeguard condition (11).

To conclude this section, we present a remark discussing the computational complexity of the AI-SSQP method, as well as its sources of randomness from both data and computation, in comparison to first-order methods. We refer the reader to [\(Na and Mahoney, 2025, Remark 4.5\)](#) for more discussions.

Remark 2.1. The AI-SSQP method relates to (unconstrained) sketched Newton methods [\(Pilanci and Wainwright, 2016, 2017; Gower and Richtárik, 2015; Gower et al., 2019; Lacotte et al., 2020, 2021; Hong et al., 2023\)](#). It is well known that solving the Newton system (6) is typically the most computationally expensive step in second-order methods. Randomized sketching solvers can significantly reduce this cost, particularly when equipped with suitable sketching matrices (e.g., sparse sketches) [\(Strohmer and Vershynin, 2008; Gower and Richtárik, 2015; Luo et al., 2016; Doikov et al., 2018; Derezhinski et al., 2020, 2021\)](#).

For first-order methods such as SGD, the per-iteration computational flops is $O(d+m)$. However, performing valid online inference is more expensive than merely achieving convergence, as it requires matrix updates to capture distributional information, resulting in the per-iteration computational cost of at least $O((d+m)^2)$. In comparison, [Na and Mahoney \(2025\)](#) showed that using sparse sketching vectors – e.g., the randomized Kaczmarz method in [Strohmer and Vershynin \(2008\)](#) samples $S \sim \text{Uniform}(\{\mathbf{e}_i\}_{i=1}^{d+m})$ – yields $O(d+m)$ flops per sketching step in (8), with $\tau = O(d+m)$ sketching steps in total to ensure the convergence of AI-SSQP. This suggests that the per-iteration cost of AI-SSQP is $O((d+m)^2)$. In our work, we further demonstrate that one can directly leverage AI-SSQP iterates to construct valid confidence intervals, thereby achieving the same $O((d+m)^2)$ cost as that required for convergence. This stands in contrast to the $O((d+m)^3)$ cost incurred by the plug-in covariance matrix estimator used in [Na and Mahoney \(2025\)](#). Therefore, our work demonstrates that AI-SSQP matches

the computational complexity of SGD for inference tasks while achieving faster convergence through second-order updates.

We highlight that AI-SSQP introduces additional sources of randomness beyond random sampling. Specifically, the sketching solver is randomized at each iteration; even with a fixed sample ξ_t , the approximate Newton direction can vary depending on the realized sketching matrices. Furthermore, the adaptive stepsize $\bar{\alpha}_t$ may be determined by the stochastic direction $(\bar{\Delta}\mathbf{x}_t, \bar{\Delta}\boldsymbol{\lambda}_t)$ and is also random. These additional layers of randomness make the uncertainty quantification analysis for AI-SSQP more challenging than that for SGD.

3 Asymptotic Normality of Averaged AI-SSQP

In this section, we first introduce the key assumptions required for the analysis of AI-SSQP, and then establish the asymptotic normality of its averaged iterate. Our assumptions are identical to (in fact, slightly weaker than) those in [Na and Mahoney \(2025\)](#), which are also standard in the existing literature. Note that the prior work investigated the asymptotic normality of the last iterate, while we complement the study by establishing the asymptotic normality of the averaged iterate. We further demonstrate that the averaged iterate exhibits better statistical efficiency, as suggested by the smaller limiting covariance matrix.

3.1 Assumptions and preliminary results

The first assumption is about constraint qualification condition and the Lipschitz continuity of the Lagrangian Hessian. These assumptions are common in constrained optimization literature ([Nocedal and Wright, 2006](#); [Bertsekas, 2014](#)).

Assumption 3.1. We assume that all the iterates $\{(\mathbf{x}_t, \boldsymbol{\lambda}_t)\}_t$ are contained in a closed, bounded, convex set $\mathcal{X} \times \Lambda$, such that $f(\mathbf{x})$ and $c(\mathbf{x})$ are twice continuously differentiable over \mathcal{X} , and the Lagrangian Hessian $\nabla^2 \mathcal{L}$ is Υ_L -Lipschitz continuous over $\mathcal{X} \times \Lambda$, that is,

$$\|\nabla^2 \mathcal{L}(\mathbf{x}, \boldsymbol{\lambda}) - \nabla^2 \mathcal{L}(\mathbf{x}', \boldsymbol{\lambda}')\| \leq \Upsilon_L \|(\mathbf{x} - \mathbf{x}', \boldsymbol{\lambda} - \boldsymbol{\lambda}')\|, \quad \forall (\mathbf{x}, \boldsymbol{\lambda}), (\mathbf{x}', \boldsymbol{\lambda}') \in \mathcal{X} \times \Lambda.$$

In addition, we assume that the Jacobian of the constraints G_t has full row rank satisfying $G_t G_t^\top \succeq \gamma_G I$ for a constant $\gamma_G > 0$. The regularization term Δ_t ensures that B_t satisfies $\|B_t\| \leq \Upsilon_B$ and $\mathbf{x}^\top B_t \mathbf{x} \geq \gamma_{RH} \|\mathbf{x}\|^2$, $\forall \mathbf{x} \in \text{Kernel}(G_t)$ for some constants $\Upsilon_B, \gamma_{RH} > 0$.

As mentioned before, the full-rank condition of G_t (known as the linear independence constraint qualification, LICQ) together with the conditions on B_t ensure that (6) has a unique solution ([Nocedal and Wright, 2006](#), Lemma 16.1). The twice continuous differentiability of $f(\mathbf{x})$ and $c(\mathbf{x})$ over the set \mathcal{X} , along with the Lipschitz continuity of the Hessian matrix $\nabla^2 \mathcal{L}$, are also standard requirements for analyzing Newton's and SQP methods.

The next assumption imposes the moment conditions on the stochastic estimates of the objective gradient and Hessian.

Assumption 3.2. We assume the gradient and Hessian estimates are unbiased: $\mathbb{E}[\nabla F(\mathbf{x}_t; \xi_t) \mid \mathbf{x}_t] = \nabla f_t$ and $\mathbb{E}[\nabla^2 F(\mathbf{x}_t; \xi_t) \mid \mathbf{x}_t] = \nabla^2 f_t$, $\forall t \geq 0$; and we assume the following moment conditions:

$$\mathbb{E}[\|\nabla F(\mathbf{x}_t; \xi_t) - \nabla f_t\|^{2+\delta} \mid \mathbf{x}_t] \leq \Upsilon_m \quad \text{and} \quad \mathbb{E}[\sup_{\mathbf{x} \in \mathcal{X}} \|\nabla^2 F(\mathbf{x}; \xi)\|^2] \leq \Upsilon_m \quad (12)$$

for some constants $\delta, \Upsilon_m > 0$.

We highlight that our inference procedure only requires a bounded $(2+\delta)$ -moment for the gradient estimates. This is weaker than existing unconstrained and constrained inference procedures that rely on covariance matrix estimation, which require *at least* a bounded fourth-order moment (Chen et al., 2020; Zhu et al., 2021; Na and Mahoney, 2025; Davis et al., 2024; Jiang et al., 2025; Kuang et al., 2025). In particular, for constrained inference problems, Na and Mahoney (2025) imposed a $(2+\delta)$ -moment condition to establish the asymptotic normality of AI-SSQP methods, and further strengthened it to a fourth-order moment condition for inference. Additionally, Davis et al. (2024) imposed a fourth-order moment condition to establish the asymptotic normality of projected SGD methods, and further strengthened it to a sub-Gaussian tail condition for valid inference.

The condition on the Hessian estimate is also standard and is required even for SGD methods (Chen et al., 2020, Assumption 3.2(2) and Lemma 3.1). It ensures the Lipschitz continuity of the mapping $\mathbf{x} \rightarrow \mathbb{E}[\nabla f(\mathbf{x}; \xi) \nabla f(\mathbf{x}; \xi)^\top]$. We note that some works may directly impose the condition on this mapping as an alternative assumption (Leluc and Portier, 2023, Assumption 4) (Davis et al., 2024, Assumption J). In fact, the Hessian condition has been shown to hold in various problems, such as least-squares and logistic regressions (Chen et al., 2020; Na and Mahoney, 2025).

The next assumption characterizes the sketching distribution, which ensures the linear convergence of the sketching solver.

Assumption 3.3. We assume the sketching matrix $S \in \mathbb{R}^{(d+m) \times q}$ satisfies $\mathbb{E}[\|S\| \|S^\dagger\|] \leq \Upsilon_S$ and

$$\mathbb{E}[K_t S (S^\top K_t^2 S)^\dagger S^\top K_t \mid \mathbf{x}_t, \boldsymbol{\lambda}_t] \succeq \gamma_S I \quad \text{for any } t \geq 0$$

for some constants $\gamma_S, \Upsilon_S > 0$.

We note that the two expectation terms above are taken over the randomness of S . The first term bounds the expected condition number of the sketching matrix, which is trivially satisfied when $q = 1$, i.e., when employing sketching vectors. The second term lower bounds the expected projection matrix, which is also standard and satisfied by various sketching methods (Gower and Richtárik, 2015). For example, for randomized Kaczmarz method with $S \sim \text{Uniform}(\{\mathbf{e}_i\}_{i=1}^{d+m})$, Na and Mahoney (2025) has shown that $\gamma_S \geq 1/\{(d+m)\kappa^2(K_t)\}$ where $\kappa(K_t)$ denotes the condition number of K_t that is uniformly upper bounded under Assumption 3.1.

With the above assumptions, we now review the global almost-sure convergence guarantee of AI-SSQP established in Na and Mahoney (2025). In nonlinear optimization, global convergence refers to the guarantee that the algorithm will converge to a stationary point from any initialization.

Theorem 3.4 (Na and Mahoney (2025), Theorem 4.8). Consider the AI-SSQP updates in (10) under Assumptions 3.1, 3.2, 3.3. There exists a threshold τ^* such that for any sketching steps $\tau \geq \tau^*$ and any stepsize control sequences $\{\beta_t, \eta_t = \beta_t + \chi_t\}$ satisfying

$$\sum_{t=0}^{\infty} \beta_t = \infty, \quad \sum_{t=0}^{\infty} \beta_t^2 < \infty, \quad \sum_{t=0}^{\infty} \chi_t < \infty, \quad (13)$$

we have $\|\nabla \mathcal{L}_t\| \rightarrow 0$ and $\|(\mathbf{x}_{t+1} - \mathbf{x}_t, \boldsymbol{\lambda}_{t+1} - \boldsymbol{\lambda}_t)\| \rightarrow 0$ as $t \rightarrow \infty$ almost surely.

The threshold τ^* has an explicit form in Na and Mahoney (2025), depending on the parameters in the presented assumptions. More specifically, $\tau^* = O(1/\log\{1/(1-\gamma_S)\}) = O(1/\gamma_S)$, suggesting that $\tau^* = O(d+m)$ when applying randomized Kaczmarz method, where $\gamma_S = O(1/(d+m))$.

Theorem 3.4 shows that AI-SSQP converges almost surely to a stationary point, which serves as the foundation for exploring the local asymptotic behavior of its iterates. To segue into the local analysis, we assume from now on that the iterates $(\mathbf{x}_t, \boldsymbol{\lambda}_t)$ converge to a *regular* local solution $(\mathbf{x}^*, \boldsymbol{\lambda}^*)$, that is, $G^* = \nabla c^*$ has full row rank and $\nabla_{\mathbf{x}}^2 \mathcal{L}^*$ is positive definite on $\text{Kernel}(G^*)$. Note that these regularity conditions are necessary even for offline M -estimators (Shapiro et al., 2014; Duchi and Ruan, 2021; Davis et al., 2024; Na and Mahoney, 2025).

3.2 Asymptotic normality

In this subsection, we examine the asymptotic normality property of the averaged AI-SSQP iterate

$$\bar{\mathbf{x}}_t = \frac{1}{t} \sum_{i=0}^{t-1} \mathbf{x}_i \quad \text{and} \quad \bar{\boldsymbol{\lambda}}_t = \frac{1}{t} \sum_{i=0}^{t-1} \boldsymbol{\lambda}_i.$$

We aim to show that, compared to the last iterate $(\mathbf{x}_t, \boldsymbol{\lambda}_t)$, the averaged iterate enjoys better efficiency. In particular, similar to the limiting covariance $\tilde{\Xi}^*$ of the last iterate (cf. (4)), the limiting covariance Ξ^* of the averaged iterate reduces to the *minimax optimal* covariance Ξ^* , achieved by the constrained M -estimators, when the sketching solver is suppressed. However, when the sketching solver is deployed, we arrive at a computational-statistical trade-off: some efficiency is lost with $\Xi^* \preceq \bar{\Xi}^* \preceq \tilde{\Xi}^*$; nevertheless, the loss is tolerable and decays exponentially in terms of the number of sketching steps: $\|\bar{\Xi}^* - \Xi^*\| \leq \|\tilde{\Xi}^* - \Xi^*\| \leq O((1 - \gamma_S)^\tau)$.

We begin by laying out the asymptotic optimality of constrained M -estimator $(\hat{\mathbf{x}}_t, \hat{\boldsymbol{\lambda}}_t)$, which generates t samples and approximates the population problem (1) by solving the empirical problem (2). Here, $\hat{\boldsymbol{\lambda}}_t$ is the associated dual solution of (2). (Shapiro et al., 2014, Chapter 5) has shown that

$$\sqrt{t} \cdot (\hat{\mathbf{x}}_t - \mathbf{x}^*, \hat{\boldsymbol{\lambda}}_t - \boldsymbol{\lambda}^*) \xrightarrow{d} \mathcal{N}(\mathbf{0}, \Xi^*)$$

with the limiting covariance Ξ^* given by

$$\Xi^* = \underbrace{\begin{pmatrix} \nabla_{\mathbf{x}}^2 \mathcal{L}^* & (G^*)^\top \\ G^* & \mathbf{0} \end{pmatrix}}_{K^* = \nabla^2 \mathcal{L}^*}^{-1} \underbrace{\begin{pmatrix} \text{cov}(\nabla F(\mathbf{x}^*; \xi)) & \mathbf{0} \\ \mathbf{0} & \mathbf{0} \end{pmatrix}}_{\text{cov}(\nabla \mathcal{L}(\mathbf{x}^*, \boldsymbol{\lambda}^*; \xi))} \underbrace{\begin{pmatrix} \nabla_{\mathbf{x}}^2 \mathcal{L}^* & (G^*)^\top \\ G^* & \mathbf{0} \end{pmatrix}}_{-1}. \quad (14)$$

Furthermore, Duchi and Ruan (2021); Davis et al. (2024) have shown that the martingale covariance of Ξ^* for the \mathbf{x} component is locally asymptotically minimax optimal in the sense of Hájek and Le Cam. Their results can be further generalized to the optimality of the full covariance Ξ^* .

For the AI-SSQP method, due to the presence of sketching steps in (8), we have to define the product of the projection matrices (projecting onto $\text{Span}(K^* S)$):

$$\tilde{C}^* := \prod_{j=1}^{\tau} (I - K^* S_j (S_j^\top (K^*)^2 S_j)^\dagger S_j^\top K^*), \quad C^* := \mathbb{E}[\tilde{C}^*] = (I - \mathbb{E}[K^* S (S^\top (K^*)^2 S)^\dagger S^\top K^*])^\tau, \quad (15)$$

where $S_1, \dots, S_\tau \stackrel{iid}{\sim} S$. The limiting covariance of AI-SSQP is adjusted from Ξ^* by these projection matrices to account for the effects of random sketching.

Theorem 3.5 (Asymptotic normality of averaged AI-SSQP). Under Assumptions 3.1, 3.2, 3.3 and suppose the sketching step $\tau \geq \tau^*$ and the stepsize control sequences $\beta_t = c_\beta/(t+1)^\beta$ and $\chi_t = c_\chi/(t+1)^\chi$ satisfy $c_\beta, c_\chi > 0$, $\beta \in (0.5, 1)$, and $\chi > \beta + 0.5$. Then, we have

$$\sqrt{t} \cdot (\bar{\mathbf{x}}_t - \mathbf{x}^*, \bar{\boldsymbol{\lambda}}_t - \boldsymbol{\lambda}^*) \xrightarrow{d} \mathcal{N}(\mathbf{0}, \bar{\Xi}^*), \quad (16)$$

where

$$\bar{\Xi}^* = (I - C^*)^{-1} \mathbb{E}[(I - \tilde{C}^*) \Xi^* (I - \tilde{C}^*)^\top] (I - C^*)^{-1}. \quad (17)$$

We mention that under Assumption 3.3, $I - C^*$ is positive definite and hence invertible, since $K^* S (S^\top (K^*)^2 S)^\dagger S^\top K^*$ is a projection matrix with a positive lower bound away from zero. Note that the conditions on the stepsize sequences $\{\beta_t, \chi_t\}$ imply the condition (13) required for the global convergence. Compared to the conditions of the normality of the last AI-SSQP iterate (Na and Mahoney, 2025, Lemma 5.12) where $\beta \in (0.5, 1]$ and $\chi > \max\{1, 1.5\beta\}$, we exclude the case $\beta = 1$. We justify this restriction from two aspects. First, for the last iterate, the optimal covariance is attained when $c_\beta = 1$, $\beta = 1$, and $\chi > 1.5$; while for the averaged iterate, the optimal covariance is attained for any $c_\beta > 0$, $\beta \in (0.5, 1)$, and $\chi > 1.5$. In practice, a smaller β (i.e., a larger stepsize) is often preferred for faster convergence. Thus, our condition enables faster convergence without compromising the optimality of the AI-SSQP method. Second, our condition generalizes the one used to analyze the (projection-based) averaged SGD method, where a deterministic stepsize is adopted ($\chi = \infty$) with $\beta \in (0.5, 1)$ (Polyak and Juditsky, 1992; Chen et al., 2020; Zhu et al., 2021; Duchi and Ruan, 2021; Davis et al., 2024).

Next, we examine in the following proposition the relationship between $\bar{\Xi}^*$ and Ξ^* .

Proposition 3.6. Under the conditions of Theorem 3.5, we have

- (a): Without the sketching solver (i.e., solving (6) exactly), $\bar{\Xi}^* = \Xi^*$.
- (b): With the sketching solver, $\bar{\Xi}^* \succeq \Xi^*$. Furthermore, their difference can be bounded by

$$\|\bar{\Xi}^* - \Xi^*\| \leq \frac{1 + (1 - \gamma_S)^\tau}{\{1 - (1 - \gamma_S)^\tau\}^2} \cdot (1 - \gamma_S)^\tau \|\Xi^*\|.$$

From the above proposition, we see that the statistical efficiency of AI-SSQP is indeed affected by the underlying sketching solver. Without sketching, the method achieves optimal statistical efficiency. With sketching, the randomized solver introduces uncertainty when solving the Newton systems, which in turn improves the method's computational efficiency. However, this comes at the cost of degraded statistical efficiency, leading to $\bar{\Xi}^* \succeq \Xi^*$. Fortunately, regardless of the sketching distribution used, the degradation remains tolerable and decays exponentially with the number of sketching steps, resulting in a favorable computational-statistical trade-off.

In the next proposition, we compare the statistical efficiency between the averaged and last iterates of AI-SSQP. Note that the computational efficiency is the same for both. In particular, Na and Mahoney (2025) has shown for $\beta \in (0.5, 1]$ and $\chi > \max\{1, 1.5\beta\}$ that

$$\sqrt{1/\beta_t} \cdot (\mathbf{x}_t - \mathbf{x}^*, \boldsymbol{\lambda}_t - \boldsymbol{\lambda}^*) \xrightarrow{d} \mathcal{N}(\mathbf{0}, \tilde{\Xi}^*), \quad (18)$$

where the limiting covariance $\tilde{\Xi}^*$ solves the following Lyapunov equation:

$$\left(\left\{ 1 - \frac{\mathbf{1}_{\{\beta=1\}}}{2c_\beta} \right\} I - C^* \right) \tilde{\Xi}^* + \tilde{\Xi}^* \left(\left\{ 1 - \frac{\mathbf{1}_{\{\beta=1\}}}{2c_\beta} \right\} I - C^* \right) = \mathbb{E}[(I - \tilde{C}^*) \Xi^* (I - \tilde{C}^*)^\top]. \quad (19)$$

To compare under the same scaling as (16), we let $\beta_t = 1/(t+1)$, corresponding to $c_\beta = 1$ and $\beta = 1$.

Proposition 3.7. Consider (19) with $c_\beta = 1$ and $\beta = 1$. If $(1 - \gamma_S)^\tau < 0.5$, then we have $\bar{\Xi}^* \preceq \tilde{\Xi}^*$.

This proposition shows that the averaged iterate exhibits better statistical efficiency than the last iterate, regardless of the sketching distribution used.

4 Online Statistical Inference

In this section, we leverage the established asymptotic normality of the averaged AI-SSQP method to perform valid online statistical inference for $(\mathbf{x}^*, \boldsymbol{\lambda}^*)$.

A direct approach is to estimate the limiting covariance to normalize the estimation error. For unconstrained strongly convex problems, Chen et al. (2020) and Zhu et al. (2021) proposed plug-in and batch-means covariance estimators, respectively, for averaged SGD methods, both of which are consistent and hence fulfill the desired goal. Kuang et al. (2025) further enhanced the covariance estimation by developing a batch-free estimator for stochastic Newton methods, and demonstrated its improved convergence rate. For constrained nonconvex problems, Na and Mahoney (2025) proposed a computationally expensive plug-in covariance estimator for $\tilde{\Xi}^*$. Due to the challenges of estimating sketching components in (19), the authors simply omitted all sketching-induced projection matrices, resulting in a biased estimator. Subsequently, Jiang et al. (2025) designed a batch-means covariance estimator for projected SGD methods to reduce computational cost. However, their analysis relies on sub-Gaussian gradient noise, a stronger condition than what is needed for establishing asymptotic normality.

The aforementioned literature motivates us to develop a valid inference procedure for the constrained problem (1) that (i) matches the computational cost of first-order methods and (ii) does not impose stronger moment conditions on the gradient noise. To this end, we leverage the random scaling technique to studentize the estimation error, rendering the limiting distribution free of any unknown quantities. As a result, we can bypass the need for covariance matrix estimation.

As the first step, we extend the normality in Theorem 3.5 to the Functional Central Limit Theorem (FCLT).

Theorem 4.1. Under the conditions of Theorem 3.5, we have

$$\frac{1}{\sqrt{t}} \sum_{i=0}^{\lfloor rt \rfloor - 1} (\mathbf{x}_i - \mathbf{x}^*, \boldsymbol{\lambda}_i - \boldsymbol{\lambda}^*) \Rightarrow (\bar{\Xi}^*)^{1/2} W_{d+m}(r), \quad r \in [0, 1],$$

where $W_{d+m}(\cdot)$ is the standard $(d + m)$ -dimensional Brownian motion and $\bar{\Xi}^*$ is defined in (17).

Here, we use “ \Rightarrow ” to denote convergence in distribution in a function space, which distinguishes it from pointwise notation \xrightarrow{d} . Specifically, $X_t(r) \Rightarrow X(r)$, $r \in [0, 1]$ if for any bounded and continuous functional $f : C[0, 1] \rightarrow \mathbb{R}$, we have $\mathbb{E}[f(X_t)] \rightarrow \mathbb{E}[f(X)]$ as $t \rightarrow \infty$, where $C[0, 1]$ denotes the space of continuous function on $[0, 1]$.

Theorem 3.5 is a special case of Theorem 4.1 with $r = 1$. The statement of Theorem 4.1 resembles the FCLT established for unconstrained SGD methods (Lee et al., 2022; Wei et al., 2023; Luo et al., 2022; Chen et al., 2024), differing mainly in the sketching-dependent scaling matrix $\bar{\Xi}^*$. However, two technical challenges arise in our constrained second-order method. First, the update rule (10) is more complex than that of standard SGD, involving not only data randomness but also computational randomness (i.e., sketching) and adaptive stepsizes. We show in the proof that the randomness from adaptive stepsizes contributes only to higher-order errors, provided that the adaptivity gap satisfies

$\chi_t = o(\beta_t/\sqrt{t})$, while the randomness from sketching is captured by the scaling matrix. Second, the Lagrangian function $\mathcal{L}(\mathbf{x}, \boldsymbol{\lambda}) = f(\mathbf{x}) + \boldsymbol{\lambda}^\top c(\mathbf{x})$ exhibits only a saddle-point structure. In contrast to the global convexity structure leveraged in prior works, we have to develop a stopping-time technique to localize our analysis (see Lemma C.1). In particular, we demonstrate that within a neighborhood of $(\mathbf{x}^*, \boldsymbol{\lambda}^*)$, the AI-SSQP iterates converge at a desirable rate, which together with the global almost-sure convergence guarantee ensures that the additional randomness does not degrade the limiting behavior of the partial sum process.

With Theorem 4.1, we now introduce a studentized, pivotal test statistic for online inference. We first define the *random scaling* matrix as

$$V_t := \frac{1}{t^2} \sum_{i=1}^t i^2 \begin{pmatrix} \bar{\mathbf{x}}_i - \bar{\mathbf{x}}_t \\ \bar{\boldsymbol{\lambda}}_i - \bar{\boldsymbol{\lambda}}_t \end{pmatrix} \begin{pmatrix} \bar{\mathbf{x}}_i - \bar{\mathbf{x}}_t \\ \bar{\boldsymbol{\lambda}}_i - \bar{\boldsymbol{\lambda}}_t \end{pmatrix}^\top.$$

Note that the matrix V_t is *not* intended to estimate the covariance $\bar{\Xi}^*$. Instead, by the continuous mapping theorem (Whitt, 2002, Theorem 3.4.3), we are able to show the following limiting distribution for the test statistic.

Theorem 4.2. Under the conditions of Theorem 3.5 and assuming $\text{cov}(\nabla F(\mathbf{x}^*; \xi)) \succ 0$, for any vector $\mathbf{w} = (\mathbf{w}_x, \mathbf{w}_\lambda) \in \mathbb{R}^{d+m}$ with $\mathbf{w} \notin \text{Span}((G^*)^\top) \otimes \mathbf{0}_m$, we have

$$\frac{\sqrt{t} \mathbf{w}^\top (\bar{\mathbf{x}}_t - \mathbf{x}^*, \bar{\boldsymbol{\lambda}}_t - \boldsymbol{\lambda}^*)}{\sqrt{\mathbf{w}^\top V_t \mathbf{w}}} \xrightarrow{d} \frac{W_1(1)}{\sqrt{\int_0^1 (W_1(r) - rW_1(1))^2 dr}}, \quad (20)$$

where $W_1(\cdot)$ is the standard one-dimensional Brownian motion.

We should mention that the condition $\mathbf{w} \notin \text{Span}((G^*)^\top) \otimes \mathbf{0}_m$ is imposed to ensure that the inference direction is not aligned with the normal direction of the constraint function, along which the variance is zero — the projection of the model parameter \mathbf{x}^* onto any normal directions $\text{Span}((G^*)^\top) = \text{Span}((\nabla c^*)^\top)$ is always zero. In particular, due to the presence of the constraints $c(\mathbf{x}) = \mathbf{0}$, the covariance matrix Ξ^* in (14) is singular. We can show that for any $\mathbf{w} = (\mathbf{w}_x, \mathbf{w}_\lambda)$ with $\mathbf{w}_x \in \text{Span}((G^*)^\top)$ and $\mathbf{w}_\lambda = \mathbf{0}$, we have $\mathbf{w}^\top \Xi^* \mathbf{w} = 0$, and vice versa. This indicates that only inference along the tangential direction $\text{Kernel}(G^*)$ is needed and non-trivial.

Theorem 4.2 shows that our test statistic is asymptotically pivotal, meaning its limiting distribution is free of any unknown parameters. In fact, the distribution in (20) appears widely in econometrics and statistics literature, such as in cointegration analysis (Johansen, 1991; Abadir and Paruolo, 1997) and robust inference (Kiefer et al., 2000; Abadir and Paruolo, 2002). For reference, we report its quantiles from Abadir and Paruolo (1997) in Table 1.

p	90%	95%	97.5%	99%
Quantile(p)	3.875	5.323	6.747	8.613

Table 1: Quantile table of the distribution $W_1(1)/\{\int_0^1 (W_1(r) - rW_1(1))^2 dr\}^{1/2}$.

Theorem 4.2 directly leads to the following corollary, which demonstrates the construction of asymptotically valid confidence intervals for $(\mathbf{x}^*, \boldsymbol{\lambda}^*)$.

Corollary 4.3. Under the conditions of Theorem 4.2, for any $p \in (0, 1)$, we have

$$P \left(\mathbf{w}^\top (\mathbf{x}^*, \boldsymbol{\lambda}^*) \in \left[\mathbf{w}^\top (\bar{\mathbf{x}}_t, \bar{\boldsymbol{\lambda}}_t) \pm U_{1-p/2} \sqrt{\mathbf{w}^\top V_t \mathbf{w} / t} \right] \right) \longrightarrow 1 - p \quad \text{as} \quad t \rightarrow \infty,$$

where $U_{1-p/2}$ denotes the $(1 - p/2) \times 100\%$ quantile of the limiting distribution in (20).

To conclude this section, we highlight that our entire inference procedure can be carried out in an online, matrix-free manner, with a computational cost of $O((d+m)^2)$, matching that of unconstrained first-order methods (Chen et al., 2020; Zhu et al., 2021). Furthermore, in contrast to existing constrained inference procedures (Na and Mahoney, 2025; Jiang et al., 2025), our approach avoids computing the projection operators and matrix inversions. Importantly, the random scaling matrix V_t can be computed in a recursive way. To see this, we rewrite V_t as follows:

$$\begin{aligned} V_t &= \frac{1}{t^2} \sum_{i=1}^t i^2 \begin{pmatrix} \bar{\mathbf{x}}_i - \bar{\mathbf{x}}_t \\ \bar{\boldsymbol{\lambda}}_i - \bar{\boldsymbol{\lambda}}_t \end{pmatrix} \begin{pmatrix} \bar{\mathbf{x}}_i - \bar{\mathbf{x}}_t \\ \bar{\boldsymbol{\lambda}}_i - \bar{\boldsymbol{\lambda}}_t \end{pmatrix}^\top \\ &= \frac{1}{t^2} \sum_{i=1}^t i^2 \begin{pmatrix} \bar{\mathbf{x}}_i \\ \bar{\boldsymbol{\lambda}}_i \end{pmatrix} \begin{pmatrix} \bar{\mathbf{x}}_i \\ \bar{\boldsymbol{\lambda}}_i \end{pmatrix}^\top - \frac{1}{t^2} \left(\sum_{i=1}^t i^2 \bar{\mathbf{x}}_i \right) \begin{pmatrix} \bar{\mathbf{x}}_t \\ \bar{\boldsymbol{\lambda}}_t \end{pmatrix}^\top - \frac{1}{t^2} \left(\bar{\mathbf{x}}_t \right) \left(\sum_{i=1}^t i^2 \bar{\mathbf{x}}_i \right)^\top + \frac{\sum_{i=1}^t i^2}{t^2} \begin{pmatrix} \bar{\mathbf{x}}_t \\ \bar{\boldsymbol{\lambda}}_t \end{pmatrix} \begin{pmatrix} \bar{\mathbf{x}}_t \\ \bar{\boldsymbol{\lambda}}_t \end{pmatrix}^\top. \end{aligned}$$

Each of the four terms above can be easily computed recursively. We formalize the online calculation in the following algorithm.

Algorithm 1 Online computation of the scaling matrix V_t

- 1: **Initialize:** set initial values for $\mathbf{s}_0 = (\mathbf{x}_0, \boldsymbol{\lambda}_0)$, $\bar{\mathbf{s}}_1 = \mathbf{s}_0$, $P_1 = \bar{\mathbf{s}}_1 \bar{\mathbf{s}}_1^\top$, $Q_1 = \bar{\mathbf{s}}_1$, $V_1 = 0$;
- 2: **for** $t = 1, 2, \dots$ **do**
- 3: Run AI-SSQP with the update (10) to obtain $\mathbf{s}_t = (\mathbf{x}_t, \boldsymbol{\lambda}_t)$;
- 4: Compute $\bar{\mathbf{s}}_{t+1} = \frac{1}{t+1} \mathbf{s}_t + \frac{t}{t+1} \bar{\mathbf{s}}_t$, $P_{t+1} = (t+1)^2 \bar{\mathbf{s}}_{t+1} \bar{\mathbf{s}}_{t+1}^\top + P_t$, $Q_{t+1} = (t+1)^2 \bar{\mathbf{s}}_{t+1} + Q_t$;
- 5: Output $V_{t+1} = \frac{1}{(t+1)^2} P_{t+1} - \frac{1}{(t+1)^2} Q_{t+1} \bar{\mathbf{s}}_{t+1}^\top - \frac{1}{(t+1)^2} \bar{\mathbf{s}}_{t+1} Q_{t+1}^\top + \frac{(t+2)(2t+3)}{6(t+1)} \bar{\mathbf{s}}_{t+1} \bar{\mathbf{s}}_{t+1}^\top$;
- 6: **end for**

5 Numerical Experiments

In this section, we demonstrate the empirical performance of our proposed inference procedure on both constrained linear and logistic regression problems. We refer our method to as **AveRS**. We compare it with four other online inference procedures based on asymptotic normality with different covariance estimators. Two procedures perform inference using the averaged AI-SSQP iterates: one employs the plug-in covariance estimator (adapted from Na and Mahoney (2025)) (**AvePlugIn**) and one employs the batch-means covariance estimator (Zhu et al., 2021) (**AveBM**). The other two procedures perform inference using the last AI-SSQP iterates: one employs the plug-in covariance estimator (Na and Mahoney, 2025) (**LastPlugIn**) and one employs the batch-free covariance estimator (Kuang et al., 2025) (**LastBF**). We note that, although the batch-means and batch-free covariance estimators are not originally proposed for the AI-SSQP methods considered here, those estimation procedures can still be readily adapted for a reasonable comparison.

We evaluate the performance of all methods by reporting the primal-dual mean absolute error, the coverage rate and length of the confidence intervals, as well as the floating-point operations (flops) per iteration required for inference.

5.1 Experimental setup

For the constrained linear regression problem, we consider the model $\xi_b = \xi_a^\top \mathbf{x}^* + \varepsilon$, where $\xi = (\xi_a, \xi_b) \in \mathbb{R}^{d+1}$ is the covariate-response pair; $\varepsilon \sim \mathcal{N}(0, \sigma^2)$ is the Gaussian noise; and $\mathbf{x}^* \in \mathbb{R}^d$ is the model parameter. For this model, we consider the squared loss function $F(\mathbf{x}; \xi) = 0.5(\xi_b - \xi_a^\top \mathbf{x})^2$. We also enforce both linear constraint $A\mathbf{x} = \mathbf{b}$ and nonlinear constraint $\|\mathbf{x}\|^2 = R^2$. Thus, the constrained linear regression problem can be summarized as:

$$\min_{\mathbf{x} \in \mathbb{R}^d} \mathbb{E} \left[\frac{1}{2} (\xi_b - \xi_a^\top \mathbf{x})^2 \right] \quad \text{s.t.} \quad A\mathbf{x} = \mathbf{b}, \quad \|\mathbf{x}\|^2 = R^2.$$

For the constrained logistic regression problem, we consider the model $P(\xi_b | \xi_a) = \frac{\exp(\xi_b \cdot \xi_a^\top \mathbf{x}^*)}{1 + \exp(\xi_b \cdot \xi_a^\top \mathbf{x}^*)}$, where $(\xi_a, \xi_b) \in \mathbb{R}^d \times \{-1, 1\}$ is the covariate-response pair and $\mathbf{x}^* \in \mathbb{R}^d$ is the model parameter. For this model, we use the log loss function $F(\mathbf{x}; \xi) = \log(1 + \exp(-\xi_b \cdot \xi_a^\top \mathbf{x}))$. Similar to the linear regression problem, we consider both linear and nonlinear constraints, arriving at

$$\min_{\mathbf{x} \in \mathbb{R}^d} \mathbb{E} \left[\log \left(1 + \exp(-\xi_b \cdot \xi_a^\top \mathbf{x}) \right) \right] \quad \text{s.t.} \quad A\mathbf{x} = \mathbf{b}, \quad \|\mathbf{x}\|^2 = R^2.$$

- **Model parameters setup.** For both regression problems, we vary the dimension $d \in \{5, 20, 40\}$ and let the true model parameter $\mathbf{x}^* \in \mathbb{R}^d$ be linearly spanned between 0 and 1. For the linear model, we let the noise variance $\sigma^2 = 1$. For each dimension, we follow the study [Na and Mahoney \(2025\)](#) and generate the covariate $\xi_a \sim \mathcal{N}(\mathbf{0}, 5I + \Sigma_a)$ with three different types of Σ_a . (i) Identity matrix: $\Sigma_a = I$; (ii) Toeplitz matrix: $[\Sigma_a]_{i,j} = r^{|i-j|}$ with $r \in \{0.4, 0.5, 0.6\}$; and (iii) Equi-correlation matrix: $[\Sigma_a]_{i,i} = 1$ and $[\Sigma_a]_{i,j} = r$ for $i \neq j$, with $r \in \{0.1, 0.2, 0.3\}$. Given ξ_a , the response ξ_b is generated by following the particular linear or logistic models. For constraints, we let $A \in \mathbb{R}^{m \times d}$ with each entry independently drawn from the standard normal distribution. We set $\mathbf{b} = A\mathbf{x}^*$, $R = \|\mathbf{x}^*\|$, and $m = 1$ for $d = 5$ and $m = 3$ otherwise.

- **Algorithm parameters setup.** All five inference procedures are based on the same AI-SSQP iteration sequence under the same algorithmic setup. In our experiment, we vary the sketching steps $\tau \in \{20, 40, \infty\}$, where $\tau = \infty$ corresponds to using the exact solver for (6). For the sketching solver, we implement the randomized Kaczmarz method ([Strohmer and Vershynin, 2008](#)); specifically, the sketching vectors are drawn from $S \sim \text{Uniform}(\{\mathbf{e}_i\}_{i=1}^{d+m})$ (cf. Section 3.1). We set $\beta_t = 1/(t+1)^{0.501}$, $\chi_t = \beta_t^2$, and choose the random stepsize $\bar{\alpha}_t \sim \text{Uniform}[\beta_t, \eta_t]$ with $\eta_t = \beta_t + \chi_t$. For the plug-in and batch-free covariance estimators, there are no additional tuning parameters beyond those in the algorithm. For the batch-means covariance estimator, we follow the setup from [Zhu et al. \(2021\)](#), setting the batch size sequence as $a_m = \lfloor m^{2/(1-\beta)} \rfloor$ with $\beta = 0.501$ (in their notation). For all inference methods, we initialize $(\mathbf{x}_0, \boldsymbol{\lambda}_0)$ as vectors of all ones and run 10^5 iterations. The nominal coverage probability $1 - p$ is set to 95%, and we conduct statistical inference for the coordinate-wise average of the model parameter, $\sum_{i=1}^d \mathbf{x}_i^*/d$. To report the confidence interval lengths and coverage rates, we conduct 200 independent runs for each parameter configuration.

5.2 Numerical results

We first investigate the consistency of the AI-SSQP iterates. In particular, we compare the estimation error of the averaged iterate $\|\bar{\mathbf{x}}_t - \mathbf{x}^*\|$ with that of the last iterate $\|\mathbf{x}_t - \mathbf{x}^*\|$. We take $d = 20$ and use the Equi-correlation design with $r = 0.2$ as a representative example, and present the comparisons under varying sketching steps in Figure 1 (similar patterns are observed across all other settings). From

the figure, we observe that the error curves of the averaged iterate decay significantly faster than those of the last iterate. This is because as shown in Theorem 3.5, the averaged iterate enjoys \sqrt{t} -consistency while the last iterate only enjoys $\sqrt{1/\beta_t} \approx O(t^{1/4})$ -consistency (see (18)). Furthermore, the larger fluctuations in the error curves of the last iterate, compared to the smoother error decay of the averaged iterate, indicate higher variability and thus lower statistical efficiency of the last iterate.

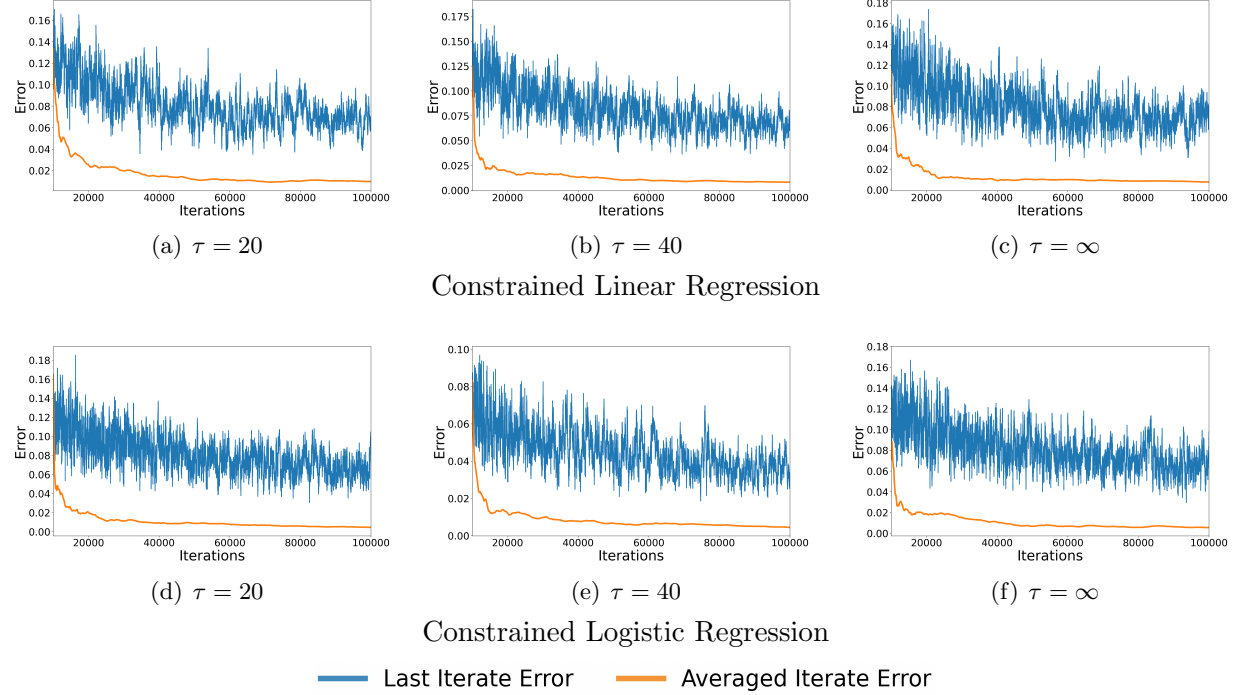


Figure 1: The averaged iterate error $\|\bar{x}_t - \mathbf{x}^*\|$ and the last iterate error $\|\mathbf{x}_t - \mathbf{x}^*\|$ for constrained linear and logistic regression with varying sketching steps τ . We use $d = 20$ and Equi-correlation design with $r = 0.2$ as an illustrative example.

Next, we investigate the empirical performance of our random scaling inference procedure alongside four other inference methods that employ different covariance matrix estimators. Among the five methods, two are based on the last iterate (**LastPlugIn**, **LastBF**), and three are based on the averaged iterate (**AvePlugIn**, **AveBM**, **AveRS** (ours)). We report the primal-dual mean absolute errors, $\|(\mathbf{x}_t - \mathbf{x}^*, \boldsymbol{\lambda}_t - \boldsymbol{\lambda}^*)\|$ for the last iterate and $\|(\bar{\mathbf{x}}_t - \mathbf{x}^*, \bar{\boldsymbol{\lambda}}_t - \boldsymbol{\lambda}^*)\|$ for the averaged iterate, along with the coverage rates and lengths of their constructed confidence intervals over 200 independent runs. We also compare the flops per iteration for different inference procedures. We summarize a subset of the results in Table 2, while the complete results and detailed discussions are provided in Appendix D.

• **Mean absolute error.** From Table 2, we observe that the averaged iterate error improves upon the last iterate error by 0.5-1 order of magnitude across all cases. As explained, this is expected since the averaged iterate achieves \sqrt{t} -consistency for any stepsize control sequence $\beta_t = O(1/t^\beta)$ with $\beta \in (0.5, 1)$, while the last iterate only achieves $O(1/\sqrt{\beta_t})$ -consistency (which is $O(t^{1/4})$ in our experiments). In fact, it is known that setting $\beta = 0.5$ (i.e., using a larger stepsize) achieves the optimal non-asymptotic algorithmic convergence rate for stochastic methods, while setting $\beta = 1$ (i.e., using a

smaller stepsize) achieves the optimal asymptotic statistical efficiency. In practice, however, setting $\beta = 1$ often leads to significantly slower convergence, making it difficult to observe optimal asymptotic normality and to perform reliable inference. In contrast, using the averaged iterate for inference allows setting $\beta \approx 0.5$ without sacrificing efficiency.

- **Asymptotic validity.** In terms of the averaged coverage rate (Ave Cov), Table 2 shows that our random scaling method consistently achieves promising coverage rates, generally close to 95% across the majority of scenarios. One exception arises in constrained linear regression when $d = 40$ and the design covariance Σ_a is Equi-correlation with $r = 0.2$: here, applying the random scaling method to exact SSQP iterates ($\tau = \infty$) leads to an overcoverage of 99%. Nevertheless, on the more computationally efficient inexact, sketched SSQP iterates ($\tau = 40$), the coverage rate improves to 96.5%.

We compare **AveRS** with other inference procedures that leverage different covariance estimators. We observe that the plug-in covariance estimators, **LastPlugIn** and **AvePlugIn**, perform reasonably well for exact SSQP iterates ($\tau = \infty$) – albeit with significantly higher computational costs – but tend to fail for inexact SSQP iterates ($\tau = 40$). This is because the plug-in estimators neglect all sketching-related components in the limiting covariance (cf. (17) and (19)), leading to inconsistency under inexact iterations. For example, in both constrained linear and logistic regression with $d = 40$ and identity design, **LastPlugIn** and **AvePlugIn** exhibit undercoverage (below 90%) for inexact SSQP, whereas **AveRS** still maintains reasonable performance. Furthermore, we note that **LastBF** is generally as competitive as **AveRS** in terms of coverage rate; however, it suffers from larger mean absolute errors and produces significantly wider confidence intervals. In addition, the existing analysis of the batch-free covariance estimator relies on the strong convexity of the problem, so the theoretical foundations for its performance in our setting remain unclear (Kuang et al., 2025). Finally, we observe that the batch-means estimator **AveBM** exhibits coverage rates far below 95%. This poor performance may be attributed to the complexity of our constrained online inference tasks and the nonconvexity of the problem, as existing analyses for this estimator often assume sub-Gaussian noise and/or strongly convex objectives (Zhu et al., 2021; Jiang et al., 2025).

- **Statistical efficiency.** In terms of the averaged confidence interval length (Ave Len), we observe that **AvePlugIn** and **AveBM** yield the shortest confidence intervals, closely followed by **AveRS**. In contrast, **LastPlugIn** and **LastBF** yield much wider intervals – by an order of magnitude – than the other three inference methods based on the averaged iterate. This pattern aligns with our observations for mean absolute error, further supporting the efficiency of averaged iterates. While **AvePlugIn** and **AveBM** benefit from the asymptotic normality of the averaged iterates, achieving minimax optimal efficiency, we emphasize that **AveRS** attains a comparable interval length while substantially improving their coverage rates since their covariance estimators are unreliable. This highlights the strength of the random scaling method with a pivotal asymptotic distribution.

- **Computational efficiency.** In terms of flops per iteration, we observe that **AveRS**, along with **AveBM** and **LastBF**, incurs the lowest computational costs, while the methods with plug-in covariance estimators (**LastPlugIn** and **AvePlugIn**) are much more expensive. This is because the plug-in estimators require computing a matrix inverse with flops $O((d+m)^3)$. In addition, AI-SSQP methods are more computationally efficient than exact SSQP methods, as the latter must solve the Newton system that involves another costly matrix inversion. Overall, AI-SSQP methods combined with the random scaling technique result in matrix-free inference procedures, making them particularly promising for considered second-order methods and matching the cost of projection-based first-order methods.

d	Design Cov	Method	Constrained linear regression			Constrained logistic regression			Flops/iter	
			MAE (10^{-2})	Ave Cov (%)	Ave Len (10^{-2})	MAE (10^{-2})	Ave Cov (%)	Ave Len (10^{-2})		
20	Identity	$\tau = \infty$	LastPlugIn	9.19	94.50	1.06	4.39	91.00	0.43	17632.74
			AvePlugIn	1.63	94.50	0.19	0.84	88.00	0.08	
			LastBF	9.19	94.50	1.05	4.39	93.50	0.46	14063.88
			AveBM	1.63	60.00	0.09	0.84	59.00	0.05	
			AveRS		97.50	0.29		95.00	0.14	
		$\tau = 40$	LastPlugIn	7.30	91.00	1.07	4.19	91.00	0.43	4768.87
			AvePlugIn	2.03	93.50	0.19	0.95	81.00	0.08	
			LastBF	7.30	92.50	1.09	4.19	95.00	0.47	1200.00
			AveBM		65.00	0.11	0.95	66.00	0.05	
			AveRS	2.03		96.00	0.36	95.50	0.17	
40	Toeplitz $r = 0.5$	$\tau = \infty$	LastPlugIn	8.99	96.50	1.46	4.16	91.50	0.47	17632.74
			AvePlugIn	1.67	93.50	0.26	0.78	93.50	0.08	
			LastBF	8.99	96.50	1.45	4.16	93.00	0.50	14063.88
			AveBM		63.00	0.13	0.78	58.50	0.05	
			AveRS		95.50	0.42		98.00	0.15	
		$\tau = 40$	LastPlugIn	7.31	99.00	1.46	4.01	92.00	0.47	4768.87
			AvePlugIn	2.03	93.00	0.26	0.92	86.50	0.08	
			LastBF	7.31	96.00	1.12	4.01	95.50	0.53	1200.00
			AveBM		56.00	0.12	0.92	66.00	0.06	
			AveRS	2.03		94.50	0.39	98.00	0.19	
80	Equi-Corr $r = 0.2$	$\tau = \infty$	LastPlugIn	8.92	95.00	1.40	4.07	94.50	0.43	17632.74
			AvePlugIn	1.59	96.00	0.25	0.76	92.50	0.08	
			LastBF	8.92	94.00	1.36	4.07	94.00	0.45	14063.88
			AveBM		60.50	0.12	0.76	64.00	0.04	
			AveRS	1.59	98.00	0.39		97.50	0.14	
		$\tau = 40$	LastPlugIn	7.43	99.50	1.40	3.81	94.00	0.42	4768.87
			AvePlugIn	1.93	89.50	0.25	0.87	92.00	0.08	
			LastBF	7.43	94.50	1.15	3.81	95.00	0.46	1200.00
			AveBM		57.00	0.13	0.87	70.00	0.05	
			AveRS	1.93		94.50	0.39	98.50	0.16	
160	Identity	$\tau = \infty$	LastPlugIn	10.68	97.00	0.62	5.63	95.00	0.28	106068.43
			AvePlugIn	1.93	94.00	0.11	1.07	90.00	0.05	
			LastBF	10.68	95.50	0.61	5.63	95.50	0.29	85975.21
			AveBM		60.00	0.06	1.07	59.00	0.03	
			AveRS	1.93	96.00	0.18		96.00	0.09	
		$\tau = 40$	LastPlugIn	10.19	86.00	0.62	5.16	89.50	0.28	22645.27
			AvePlugIn	2.60	81.00	0.11	1.43	78.00	0.05	
			LastBF	10.19	93.50	0.76	5.16	91.50	0.30	2552.05
			AveBM		64.00	0.08	1.43	65.00	0.04	
			AveRS	2.60		97.00	0.26	96.50	0.13	
320	Toeplitz $r = 0.5$	$\tau = \infty$	LastPlugIn	10.73	94.00	0.59	5.28	94.00	0.30	10608.43
			AvePlugIn	1.96	95.50	0.11	0.99	90.50	0.05	
			LastBF	10.73	94.00	0.58	5.28	94.00	0.31	85975.21
			AveBM		66.50	0.06	0.99	68.00	0.03	
			AveRS	1.96	94.50	0.18		96.00	0.10	
		$\tau = 40$	LastPlugIn	10.15	84.50	0.59	4.84	95.00	0.30	22645.27
			AvePlugIn	2.67	80.50	0.10	1.38	79.00	0.05	
			LastBF	10.15	95.50	0.77	4.84	92.50	0.30	2552.05
			AveBM		60.50	0.07	1.38	62.00	0.04	
			AveRS	2.67		97.00	0.23	95.50	0.12	
640	Equi-Corr $r = 0.2$	$\tau = \infty$	LastPlugIn	10.95	94.50	0.66	4.85	95.00	0.27	10608.44
			AvePlugIn	1.97	95.50	0.12	0.90	92.50	0.05	
			LastBF	10.95	94.50	0.65	4.85	95.00	0.28	85975.21
			AveBM		70.00	0.06	0.90	69.00	0.03	
			AveRS		99.00	0.19		97.00	0.09	
		$\tau = 40$	LastPlugIn	10.31	92.00	0.66	4.52	94.50	0.27	22645.27
			AvePlugIn	2.83	86.00	0.12	1.21	80.50	0.05	
			LastBF	10.31	94.50	0.78	4.52	94.50	0.27	2552.05
			AveBM		65.00	0.08	1.21	63.50	0.03	
			AveRS	2.83		96.50	0.25	96.50	0.11	

Table 2: A subset of comparison results for different inference methods on constrained linear and logistic regression problems. For each combination of dimension and design covariance, we highlight the coverage rate and confidence interval length of a method if no other method achieves a comparably good coverage rate with a shorter confidence interval. If the coverage rates and confidence lengths are comparable, we highlight the method with fewer flops per iteration.

6 Conclusion and Future Work

In this paper, we developed an online inference procedure for constrained stochastic optimization problems by leveraging a numerical method called Adaptive Inexact Stochastic Sequential Quadratic Programming (AI-SSQP). At each step, the method employs a sketching solver to approximately solve the expensive quadratic subproblem and selects a proper adaptive random stepsize. We established the asymptotic normality of the averaged SSQP iterate $(\bar{\mathbf{x}}_t, \bar{\boldsymbol{\lambda}}_t)$ and demonstrated that the averaged iterate enjoys better statistical efficiency than the last iterate, as evidenced by a smaller limiting covariance matrix. This limiting covariance reduces to the minimax optimal covariance when sketching is degraded, and, when sketching is used, remains close to the optimal covariance within a radius that decays exponentially fast in terms of the number of sketching steps. Furthermore, we analyzed the partial sum process of SSQP, $\frac{1}{\sqrt{t}} \sum_{i=0}^{\lfloor rt \rfloor - 1} (\mathbf{x}_i - \mathbf{x}^*, \boldsymbol{\lambda}_i - \boldsymbol{\lambda}^*)$, and proved that it converges in distribution to a standard Brownian motion. Based on this result, we proposed a test statistic by studentizing the estimation error $\sqrt{t} \cdot (\bar{\mathbf{x}}_t - \mathbf{x}^*, \bar{\boldsymbol{\lambda}}_t - \boldsymbol{\lambda}^*)$ using a random scaling matrix V_t . We showed that the resulting test statistic is asymptotically pivotal, in the sense that its limiting distribution is free of any unknown parameters. This enables the construction of valid confidence intervals for the local solution $(\mathbf{x}^*, \boldsymbol{\lambda}^*)$. Our random scaling method is fully online and matrix-free, significantly reducing both the computational and memory costs that typically burden second-order methods. In particular, our method matches the computational efficiency of state-of-the-art unconstrained first-order methods, making it particularly suitable for large-scale, streaming data settings.

For future research, it is of interest to design online inference procedures for inequality-constrained stochastic optimization problems. Many methods of solving inequality-constrained problems asymptotically reduce to solving equality-constrained problems, suggesting that the random scaling analysis, along with the stopping-time localization technique, can still be applicable (Na et al., 2023). In addition, recent works on online inference have extended the data sampling scheme for first-order methods from i.i.d. data to Markovian data (Li et al., 2023; Roy and Balasubramanian, 2023). A promising direction, therefore, is to adapt second-order methods to the Markovian sampling settings and establish the corresponding online inference theory. Finally, extending constrained online inference to high-dimensional settings, where the dimensionality grows with the sample size, is also an important avenue for future exploration.

References

K. M. Abadir and P. Paruolo. Two mixed normal densities from cointegration analysis. *Econometrica*, 65(3):671, 1997.

K. M. Abadir and P. Paruolo. Simple robust testing of regression hypotheses: A comment. *Econometrica*, 70(5):2097–2099, 2002.

A. S. Berahas, F. E. Curtis, D. Robinson, and B. Zhou. Sequential quadratic optimization for nonlinear equality constrained stochastic optimization. *SIAM Journal on Optimization*, 31(2):1352–1379, 2021.

A. S. Berahas, F. E. Curtis, M. J. O’Neill, and D. P. Robinson. A stochastic sequential quadratic optimization algorithm for nonlinear-equality-constrained optimization with rank-deficient jacobians. *Mathematics of Operations Research*, 49(4):2212–2248, 2024.

B. Bercu, A. Godichon, and B. Portier. An efficient stochastic Newton algorithm for parameter estimation in logistic regressions. *SIAM Journal on Control and Optimization*, 58(1):348–367, 2020.

D. P. Bertsekas. Nonlinear programming. *Journal of the Operational Research Society*, 48(3):334–334, 1997.

D. P. Bertsekas. *Constrained optimization and Lagrange multiplier methods*. Academic press, 2014.

C. Boyer and A. Godichon-Baggioni. On the asymptotic rate of convergence of stochastic newton algorithms and their weighted averaged versions. *Computational Optimization and Applications*, 84(3):921–972, 2023.

N. Chatterjee, Y.-H. Chen, P. Maas, and R. J. Carroll. Constrained maximum likelihood estimation for model calibration using summary-level information from external big data sources. *Journal of the American Statistical Association*, 111(513):107–117, 2016.

C. Chen, F. Tung, N. Vedula, and G. Mori. Constraint-aware deep neural network compression. In *Computer Vision – ECCV 2018*, pages 409–424. Springer International Publishing, 2018.

X. Chen, J. D. Lee, X. T. Tong, and Y. Zhang. Statistical inference for model parameters in stochastic gradient descent. *The Annals of Statistics*, 48(1), 2020.

X. Chen, Z. Lai, H. Li, and Y. Zhang. Online statistical inference for stochastic optimization via kiefer-wolfowitz methods. *Journal of the American Statistical Association*, 119(548):2972–2982, 2024.

S. Cuomo, V. S. Di Cola, F. Giampaolo, G. Rozza, M. Raissi, and F. Piccialli. Scientific machine learning through physics-informed neural networks: Where we are and what’s next. *Journal of Scientific Computing*, 92(3):88, 2022.

F. E. Curtis, D. P. Robinson, and B. Zhou. A stochastic inexact sequential quadratic optimization algorithm for nonlinear equality-constrained optimization. *INFORMS Journal on Optimization*, 6(3–4):173–195, 2024.

P. Cénac, A. Godichon-Baggioni, and B. Portier. An efficient averaged stochastic gauss-newton algorithm for estimating parameters of nonlinear regressions models. *Bernoulli*, 31(1), 2025.

D. Davis, D. Drusvyatskiy, S. Kakade, and J. D. Lee. Stochastic subgradient method converges on tame functions. *Foundations of Computational Mathematics*, 20(1):119–154, 2019.

D. Davis, D. Drusvyatskiy, and L. Jiang. Asymptotic normality and optimality in nonsmooth stochastic approximation. *The Annals of Statistics*, 52(4), 2024.

M. Derezhinski, B. Bartan, M. Pilanci, and M. W. Mahoney. Debiasing distributed second order optimization with surrogate sketching and scaled regularization. *Advances in Neural Information Processing Systems*, 33:6684–6695, 2020.

M. Derezhinski, J. Lacotte, M. Pilanci, and M. W. Mahoney. Newton-less: Sparsification without trade-offs for the sketched newton update. *Advances in Neural Information Processing Systems*, 34:2835–2847, 2021.

N. Doikov, P. Richtárik, et al. Randomized block cubic newton method. In *International Conference on Machine Learning*, pages 1290–1298. PMLR, 2018.

J.-H. Du, Y. Guo, and X. Wang. High-dimensional portfolio selection with cardinality constraints. *Journal of the American Statistical Association*, 118(542):779–791, 2022.

J. C. Duchi and F. Ruan. Asymptotic optimality in stochastic optimization. *The Annals of Statistics*, 49(1), 2021.

M. Duflo. *Random iterative models*, volume 34. Springer Science & Business Media, Berlin New York, 2013.

J. Fan, J. Zhang, and K. Yu. Vast portfolio selection with gross-exposure constraints. *Journal of the American Statistical Association*, 107(498):592–606, 2012.

Y. Fang, J. Xu, and L. Yang. Online bootstrap confidence intervals for the stochastic gradient descent estimator. *Journal of Machine Learning Research*, 19(78):1–21, 2018.

Y. Fang, S. Na, M. W. Mahoney, and M. Kolar. Fully stochastic trust-region sequential quadratic programming for equality-constrained optimization problems. *SIAM Journal on Optimization*, 34(2):2007–2037, 2024.

C. J. Geyer. Constrained maximum likelihood exemplified by isotonic convex logistic regression. *Journal of the American Statistical Association*, 86(415):717–724, 1991.

R. Gower, D. Kovalev, F. Lieder, and P. Richtárik. Rsn: randomized subspace newton. *Advances in Neural Information Processing Systems*, 32, 2019.

R. M. Gower and P. Richtárik. Randomized iterative methods for linear systems. *SIAM Journal on Matrix Analysis and Applications*, 36(4):1660–1690, 2015.

P. Hall and C. C. Heyde. *Martingale limit theory and its application*. Academic press, 2014.

I. Hong, S. Na, M. W. Mahoney, and M. Kolar. Constrained optimization via exact augmented lagrangian and randomized iterative sketching. In *International Conference on Machine Learning*, pages 13174–13198. PMLR, 2023.

L. Jiang, A. Roy, K. Balasubramanian, D. Davis, D. Drusvyatskiy, and S. Na. Online covariance estimation in nonsmooth stochastic approximation. *arXiv preprint arXiv:2502.05305*, 2025.

S. Johansen. Estimation and hypothesis testing of cointegration vectors in gaussian vector autoregressive models. *Econometrica*, 59(6):1551, 1991.

H. Khalil. *Nonlinear Systems*. Pearson Education. Prentice Hall, 2002.

J. Kiefer and J. Wolfowitz. Stochastic estimation of the maximum of a regression function. *The Annals of Mathematical Statistics*, 23(3):462–466, 1952.

N. M. Kiefer, T. J. Vogelsang, and H. Bunzel. Simple robust testing of regression hypotheses. *Econometrica*, 68(3):695–714, 2000.

D. P. Kouri, M. Heinkenschloss, D. Ridzal, and B. G. van Bloemen Waanders. Inexact objective function evaluations in a trust-region algorithm for pde-constrained optimization under uncertainty. *SIAM Journal on Scientific Computing*, 36(6):A3011–A3029, 2014.

W. Kuang, M. Anitescu, and S. Na. Online covariance matrix estimation in sketched newton methods. *arXiv preprint arXiv:2502.07114*, 2025.

J. Lacotte, S. Liu, E. Dobriban, and M. Pilanci. Optimal iterative sketching methods with the subsampled randomized hadamard transform. *Advances in Neural Information Processing Systems*, 33:9725–9735, 2020.

J. Lacotte, Y. Wang, and M. Pilanci. Adaptive newton sketch: Linear-time optimization with quadratic convergence and effective hessian dimensionality. In *International Conference on Machine Learning*, pages 5926–5936. PMLR, 2021.

S. Lee, Y. Liao, M. H. Seo, and Y. Shin. Fast and robust online inference with stochastic gradient descent via random scaling. In *Proceedings of the AAAI Conference on Artificial Intelligence*, volume 36, pages 7381–7389, 2022.

R. Leluc and F. Portier. Asymptotic analysis of conditioned stochastic gradient descent. *Transactions on Machine Learning Research*, 2023.

X. Li, J. Liang, and Z. Zhang. Online statistical inference for nonlinear stochastic approximation with markovian data. *arXiv preprint arXiv:2302.07690*, 2023.

H. Luo, A. Agarwal, N. Cesa-Bianchi, and J. Langford. Efficient second order online learning by sketching. In *Advances in Neural Information Processing Systems*, pages 902–910, 2016.

Y. Luo, X. Huo, and Y. Mei. Covariance estimators for the root-sgd algorithm in online learning. *arXiv preprint arXiv:2212.01259*, 2022.

S. Na and M. Mahoney. Statistical inference of constrained stochastic optimization via sketched sequential quadratic programming. *Journal of Machine Learning Research*, 26(33):1–75, 2025.

S. Na, M. Anitescu, and M. Kolar. An adaptive stochastic sequential quadratic programming with differentiable exact augmented lagrangians. *Mathematical Programming*, 199(1–2):721–791, 2022.

S. Na, M. Anitescu, and M. Kolar. Inequality constrained stochastic nonlinear optimization via active-set sequential quadratic programming. *Mathematical Programming*, 2023.

S. Na, M. Anitescu, and M. Kolar. A fast temporal decomposition procedure for long-horizon nonlinear dynamic programming. *Mathematics of Operations Research*, 49(2):1012–1044, 2024.

Y. Nandwani, A. Pathak, and P. Singla. A primal dual formulation for deep learning with constraints. *Advances in neural information processing systems*, 32, 2019.

J. Nocedal and S. J. Wright. *Numerical Optimization*. Springer New York, 2nd edition, 2006.

M. Pilanci and M. J. Wainwright. Iterative hessian sketch: Fast and accurate solution approximation for constrained least-squares. *J. Mach. Learn. Res.*, 17(1):1842–1879, 2016.

M. Pilanci and M. J. Wainwright. Newton sketch: A near linear-time optimization algorithm with linear-quadratic convergence. *SIAM Journal on Optimization*, 27(1):205–245, 2017.

B. T. Polyak and A. B. Juditsky. Acceleration of stochastic approximation by averaging. *SIAM Journal on Control and Optimization*, 30(4):838–855, 1992.

T. Rees, H. S. Dollar, and A. J. Wathen. Optimal solvers for pde-constrained optimization. *SIAM Journal on Scientific Computing*, 32(1):271–298, 2010.

H. Robbins and D. Siegmund. *A convergence theorem for non negative almost supermartingales and some applications*, pages 233–257. Elsevier, 1971.

H. Robbins and S. Monro. A stochastic approximation method. *The Annals of Mathematical Statistics*, 22(3):400–407, 1951.

A. Roy and K. Balasubramanian. Online covariance estimation for stochastic gradient descent under markovian sampling. *arXiv preprint arXiv:2308.01481*, 2023.

S. K. Roy, Z. Mhammedi, and M. Harandi. Geometry aware constrained optimization techniques for deep learning. In *Proceedings of the IEEE conference on computer vision and pattern recognition*, pages 4460–4469, 2018.

A. Shapiro, D. Dentcheva, and A. Ruszczyński. *Lectures on Stochastic Programming: Modeling and Theory, Second Edition*. Society for Industrial and Applied Mathematics, 2014.

T. Strohmer and R. Vershynin. A randomized kaczmarz algorithm with exponential convergence. *Journal of Fourier Analysis and Applications*, 15(2):262–278, 2008.

Z. Wei, W. Zhu, and W. B. Wu. Weighted averaged stochastic gradient descent: Asymptotic normality and optimality. *arXiv preprint arXiv:2307.06915*, 2023.

W. Whitt. *Stochastic-Process Limits: An Introduction to Stochastic-Process Limits and Their Application to Queues*. Springer New York, 2002.

W. Zhu, X. Chen, and W. B. Wu. Online covariance matrix estimation in stochastic gradient descent. *Journal of the American Statistical Association*, 118(541):393–404, 2021.

A Preparation Lemmas and Preliminaries

We present some preparation results that will be used in our later proofs. Throughout the sections, we use the following filtration to clearly identify the source of randomness:

$$\mathcal{F}_{t-0.5} = \sigma(\{\xi_i, \{S_{i,j}\}_j, \bar{\alpha}_i\}_{i=0}^{t-1} \cup \xi_t), \quad \mathcal{F}_t = \sigma(\{\xi_i, \{S_{i,j}\}_j, \bar{\alpha}_i\}_{i=0}^t).$$

For consistency, \mathcal{F}_{-1} denotes the trivial σ -algebra. We recall that $\tilde{\mathbf{z}}_t = (\tilde{\Delta}\mathbf{x}_t, \tilde{\Delta}\boldsymbol{\lambda}_t)$ is the exact stochastic Newton direction in (6) and $\mathbf{z}_{t,\tau} = (\bar{\Delta}\mathbf{x}_t, \bar{\Delta}\boldsymbol{\lambda}_t)$ is the sketched Newton direction in (9). For the sake of brevity, we define the following projection matrices:

$$C_{t,j} := I - K_t S_{t,j} (S_{t,j}^\top K_t^2 S_{t,j})^\dagger S_{t,j}^\top K_t, \quad \tilde{C}_t := \prod_{j=0}^{\tau-1} C_{t,j}, \quad C_t := \mathbb{E}[\tilde{C}_t \mid \mathcal{F}_{t-1}]. \quad (\text{A.1})$$

By the sketching update (8), (6), and the setup of $\mathbf{z}_{t,0} = \mathbf{0}$, we have

$$\mathbf{z}_{t,\tau} - \tilde{\mathbf{z}}_t = C_{t,\tau-1}(\mathbf{z}_{t,\tau-1} - \tilde{\mathbf{z}}_t) = \left(\prod_{j=0}^{\tau-1} C_{t,j} \right) (\mathbf{z}_{t,0} - \tilde{\mathbf{z}}_t) = -\tilde{C}_t \tilde{\mathbf{z}}_t \implies \mathbf{z}_{t,\tau} = (I - \tilde{C}_t) \tilde{\mathbf{z}}_t. \quad (\text{A.2})$$

We let $\rho := 1 - \gamma_S$, where γ_S is introduced in Assumption 3.3. The first lemma provides guarantees on the sketching solver.

Lemma A.1. Under Assumptions 3.1, 3.2, 3.3, we have for all $t \geq 0$,

- (a): $0 \leq \rho < 1$.
- (b): $\mathbb{E}[\mathbf{z}_{t,\tau} \mid \mathcal{F}_{t-0.5}] = (I - C_t) \tilde{\mathbf{z}}_t$ and $\mathbb{E}[\|\mathbf{z}_{t,\tau}\|^2 \mid \mathcal{F}_{t-1}] \leq \Upsilon_z$ for some constant $\Upsilon_z > 0$.
- (c): $\|C_t\| \leq \rho^\tau$ and $\|C_t - C^*\| \leq 2\tau\Upsilon_S\|K_t - K^*\|/\sigma_{\min}(K^*)$, where C^* is defined in (15).

Proof. (a) By Assumption 3.3, we know $\gamma_S > 0$; thus, $\rho < 1$. Further, $\gamma_S \leq \mathbb{E}[\|K_t S (S^\top K_t^2 S)^\dagger S^\top K_t\| \mid \mathbf{x}_t, \boldsymbol{\lambda}_t] \leq 1$; thus, $\rho \geq 0$. (b) The first result follows directly from (A.2) and the independence between randomness of ξ_t and $\{S_{t,j}\}_j$; the second result is from (Na and Mahoney, 2025, (D.10)). (c) The first result follows from the independence among $\{S_{t,j}\}_j$, and the second result is from (Na and Mahoney, 2025, Corollary 5.4). \blacksquare

The next lemma provides bounds and convergence results for the Hessian matrix K_t and the projection matrix C_t .

Lemma A.2. Under Assumptions 3.1, 3.2, 3.3, and assuming $(\mathbf{x}_t, \boldsymbol{\lambda}_t) \xrightarrow{a.s.} (\mathbf{x}^*, \boldsymbol{\lambda}^*)$, we have

- (a): The Hessian modification $\Delta_t = 0$ for large t , and $K_t \rightarrow K^*$, $C_t \rightarrow C^*$ as $t \rightarrow \infty$ almost surely.
- (b): There exists a constant $\Upsilon_K > 0$ such that $\|K_t^{-1}\| \leq \Upsilon_K$, $\forall t \geq 0$.

Proof. Recall K_t is defined in (6) and K^* in (14). The result (a) is from (Na and Mahoney, 2025, Lemma E.4) and Lemma A.1(c), while the result (b) is from (Na et al., 2024, Lemma 5.1). \blacksquare

We then decompose the recursion of the AI-SSQP method into several components, including the martingale difference component, the stepsize adaptivity component, and other higher-order components. These components will be analyzed separately when establishing asymptotic normality.

Lemma A.3. Let $\boldsymbol{\omega}_t = (\mathbf{x}_t - \mathbf{x}^*, \boldsymbol{\lambda}_t - \boldsymbol{\lambda}^*)$. The error recursion of AI-SSQP can be decomposed as

$$\boldsymbol{\omega}_{t+1} = \{I - \beta_t(I - C^*)\} \boldsymbol{\omega}_t + \beta_t(\boldsymbol{\theta}_t + \boldsymbol{\delta}_t) + (\bar{\alpha}_t - \beta_t) \mathbf{z}_{t,\tau},$$

where

$$\boldsymbol{\theta}_t = -(I - C_t) K_t^{-1} (\bar{\nabla} \mathcal{L}_t - \nabla \mathcal{L}_t) + \{\mathbf{z}_{t,\tau} - (I - C_t) \tilde{\mathbf{z}}_t\}, \quad (\text{A.3a})$$

$$\boldsymbol{\delta}_t = -(I - C_t) \{(K^*)^{-1} \boldsymbol{\psi}_t + \{K_t^{-1} - (K^*)^{-1}\} \nabla \mathcal{L}_t\} + (C_t - C^*) \boldsymbol{\omega}_t, \quad (\text{A.3b})$$

$$\boldsymbol{\psi}_t = \nabla \mathcal{L}_t - K^* \boldsymbol{\omega}_t, \quad (\text{A.3c})$$

and C_t is defined in (A.1), C^* in (15), K_t in (6), and K^* in (14). Furthermore, under Assumptions 3.1, 3.2, 3.3, and supposing $(\mathbf{x}_t, \boldsymbol{\lambda}_t) \rightarrow (\mathbf{x}^*, \boldsymbol{\lambda}^*)$, we know $\boldsymbol{\theta}_t$ is a martingale difference with $\mathbb{E}[\boldsymbol{\theta}_t \mid \mathcal{F}_{t-1}] = \mathbf{0}$ and

$$\mathbb{E}[\boldsymbol{\theta}_t \boldsymbol{\theta}_t^\top \mid \mathcal{F}_{t-1}] \xrightarrow{a.s.} \mathbb{E}[(I - \tilde{C}^*) \Xi^* (I - \tilde{C}^*)^\top] \quad \text{as } t \rightarrow \infty. \quad (\text{A.4})$$

Proof. From the update rule of AI-SSQP in (10), we have

$$\begin{aligned}
\boldsymbol{\omega}_{t+1} &= \boldsymbol{\omega}_t + \bar{\alpha}_t \boldsymbol{z}_{t,\tau} = \boldsymbol{\omega}_t + \beta_t \boldsymbol{z}_{t,\tau} + (\bar{\alpha}_t - \beta_t) \boldsymbol{z}_{t,\tau} \\
&= \boldsymbol{\omega}_t + \beta_t (I - C_t) \tilde{\boldsymbol{z}}_t + \beta_t \{ \boldsymbol{z}_{t,\tau} - (I - C_t) \tilde{\boldsymbol{z}}_t \} + (\bar{\alpha}_t - \beta_t) \boldsymbol{z}_{t,\tau} \\
&\stackrel{(6)}{=} \boldsymbol{\omega}_t - \beta_t (I - C_t) K_t^{-1} \bar{\nabla} \mathcal{L}_t + \beta_t \{ \boldsymbol{z}_{t,\tau} - (I - C_t) \tilde{\boldsymbol{z}}_t \} + (\bar{\alpha}_t - \beta_t) \boldsymbol{z}_{t,\tau} \\
&= \boldsymbol{\omega}_t - \beta_t (I - C_t) K_t^{-1} \nabla \mathcal{L}_t - \beta_t (I - C_t) K_t^{-1} (\bar{\nabla} \mathcal{L}_t - \nabla \mathcal{L}_t) + \beta_t \{ \boldsymbol{z}_{t,\tau} - (I - C_t) \tilde{\boldsymbol{z}}_t \} + (\bar{\alpha}_t - \beta_t) \boldsymbol{z}_{t,\tau} \\
&\stackrel{(A.3a)}{=} \boldsymbol{\omega}_t - \beta_t (I - C_t) K_t^{-1} \nabla \mathcal{L}_t + \beta_t \boldsymbol{\theta}_t + (\bar{\alpha}_t - \beta_t) \boldsymbol{z}_{t,\tau} \tag{A.5} \\
&= \boldsymbol{\omega}_t - \beta_t (I - C_t) (K^*)^{-1} \nabla \mathcal{L}_t - \beta_t (I - C_t) \{ K_t^{-1} - (K^*)^{-1} \} \nabla \mathcal{L}_t + \beta_t \boldsymbol{\theta}_t + (\bar{\alpha}_t - \beta_t) \boldsymbol{z}_{t,\tau} \\
&\stackrel{(A.3c)}{=} \{ I - \beta_t (I - C_t) \} \boldsymbol{\omega}_t - \beta_t (I - C_t) (K^*)^{-1} \boldsymbol{\psi}_t - \beta_t (I - C_t) \{ K_t^{-1} - (K^*)^{-1} \} \nabla \mathcal{L}_t \\
&\quad + \beta_t \boldsymbol{\theta}_t + (\bar{\alpha}_t - \beta_t) \boldsymbol{z}_{t,\tau} \\
&\stackrel{(A.3b)}{=} \{ I - \beta_t (I - C^*) \} \boldsymbol{\omega}_t + \beta_t (\boldsymbol{\theta}_t + \boldsymbol{\delta}_t) + (\bar{\alpha}_t - \beta_t) \boldsymbol{z}_{t,\tau}.
\end{aligned}$$

Moreover, by Assumption 3.2 and Lemma A.1(b), we have $\mathbb{E}[\boldsymbol{\theta}_t | \mathcal{F}_{t-1}] = \mathbf{0}$. The result (A.4) is established in Na and Mahoney (2025) after (E.15). This completes the proof. \blacksquare

Lemma A.4 (Davis et al. (2024), Lemma A.9). Suppose $\{A_t\}_t$ is a non-negative sequence satisfying

$$A_{t+1} \leq (1 - c_1 t^{-\beta}) A_t + c_2 t^{-2\beta}, \quad \forall t \geq t_0,$$

for some constants $c_1, c_2 > 0$, $\beta \in (0.5, 1)$, and positive integer t_0 . Then, there exists a constant $c_0 > 0$ such that $A_t \leq c_0 t^{-\beta}$ for all $t \geq 1$.

Lemma A.5 (Kronecker's lemma). Suppose $\{A_t\}_t$ is a sequence such that $\sum_{t=0}^{\infty} A_t$ exists and is finite. For any divergent positive non-decreasing sequence $\{a_t\}_t$, we have $\frac{1}{a_T} \sum_{t=1}^T a_t A_t \rightarrow 0$ as $T \rightarrow \infty$.

B Proofs of Main Theorems

B.1 Proof of Theorem 3.5

By Lemma A.1(a), (c), and Lemma A.2(a), we know $\|C^*\| \leq \rho < 1$. Thus, $I - C^*$ is a positive definite and, thus, invertible matrix. Let us define two matrices

$$B_i^t = \beta_i \sum_{k=i}^t \prod_{j=i+1}^k (I - \beta_j (I - C^*)) \quad \text{and} \quad A_i^t = B_i^t - (I - C^*)^{-1}. \tag{B.1}$$

Recall that $\boldsymbol{\omega}_k = (\boldsymbol{x}_k - \boldsymbol{x}^*, \boldsymbol{\lambda}_k - \boldsymbol{\lambda}^*)$. We apply Lemma A.3 recursively and obtain

$$\boldsymbol{\omega}_{k+1} = \prod_{j=0}^k (I - \beta_j (I - C^*)) \boldsymbol{\omega}_0 + \sum_{i=0}^k \prod_{j=i+1}^k (I - \beta_j (I - C^*)) \beta_i \left(\boldsymbol{\theta}_i + \boldsymbol{\delta}_i + \frac{\bar{\alpha}_i - \beta_i}{\beta_i} \boldsymbol{z}_{i,\tau} \right).$$

Therefore, we obtain

$$\begin{aligned}
& \frac{1}{\sqrt{t}} \sum_{k=1}^t \boldsymbol{\omega}_k \\
&= \frac{1}{\sqrt{t}} \sum_{k=0}^{t-1} \prod_{j=0}^k (I - \beta_j(I - C^*)) \boldsymbol{\omega}_0 + \frac{1}{\sqrt{t}} \sum_{k=0}^{t-1} \sum_{i=0}^k \prod_{j=i+1}^k (I - \beta_j(I - C^*)) \beta_i \left(\boldsymbol{\theta}_i + \boldsymbol{\delta}_i + \frac{\bar{\alpha}_i - \beta_i}{\beta_i} \mathbf{z}_{i,\tau} \right) \\
&\stackrel{(B.1)}{=} \frac{1}{\sqrt{t}\beta_0} B_0^{t-1} (I - \beta_0(I - C^*)) \boldsymbol{\omega}_0 + \frac{1}{\sqrt{t}} \sum_{i=0}^{t-1} \sum_{k=i}^{t-1} \prod_{j=i+1}^k (I - \beta_j(I - C^*)) \beta_i \left(\boldsymbol{\theta}_i + \boldsymbol{\delta}_i + \frac{\bar{\alpha}_i - \beta_i}{\beta_i} \mathbf{z}_{i,\tau} \right) \\
&\stackrel{(B.1)}{=} \frac{1}{\sqrt{t}\beta_0} B_0^{t-1} (I - \beta_0(I - C^*)) \boldsymbol{\omega}_0 + \frac{1}{\sqrt{t}} \sum_{i=0}^{t-1} B_i^{t-1} \left(\boldsymbol{\theta}_i + \boldsymbol{\delta}_i + \frac{\bar{\alpha}_i - \beta_i}{\beta_i} \mathbf{z}_{i,\tau} \right) \\
&\stackrel{(B.1)}{=} \frac{1}{\sqrt{t}\beta_0} B_0^{t-1} (I - \beta_0(I - C^*)) \boldsymbol{\omega}_0 + \frac{1}{\sqrt{t}} \sum_{i=0}^{t-1} B_i^{t-1} \left(\boldsymbol{\delta}_i + \frac{\bar{\alpha}_i - \beta_i}{\beta_i} \mathbf{z}_{i,\tau} \right) + \frac{1}{\sqrt{t}} \sum_{i=0}^{t-1} A_i^{t-1} \boldsymbol{\theta}_i \\
&\quad + \frac{1}{\sqrt{t}} \sum_{i=0}^{t-1} (I - C^*)^{-1} \boldsymbol{\theta}_i. \tag{B.2}
\end{aligned}$$

In what follows, we analyze each right-hand-side term above and establish the following claims:

- (a): $\frac{1}{\sqrt{t}} \sum_{i=0}^{t-1} (I - C^*)^{-1} \boldsymbol{\theta}_i \xrightarrow{d} \mathcal{N}(0, \bar{\Xi}^*)$, where $\bar{\Xi}^*$ is defined in (17).
- (b): $\frac{1}{\sqrt{t}} \sum_{i=0}^{t-1} A_i^{t-1} \boldsymbol{\theta}_i = o_p(1)$.
- (c): $\frac{1}{\sqrt{t}} \sum_{i=0}^{t-1} B_i^{t-1} \boldsymbol{\delta}_i = o(1)$.
- (d): $\frac{1}{\sqrt{t}} \sum_{i=0}^{t-1} B_i^{t-1} \frac{(\bar{\alpha}_i - \beta_i)}{\beta_i} \mathbf{z}_{i,\tau} = o(1)$.
- (e): $\frac{1}{\sqrt{t}\beta_0} B_0^{t-1} [I - \beta_0(I - C^*)] \boldsymbol{\omega}_0 = o(1)$.

Combining these claims together, we obtain

$$\frac{1}{\sqrt{t}} \sum_{k=1}^t \boldsymbol{\omega}_k \xrightarrow{d} \mathcal{N}(0, \bar{\Xi}^*).$$

This completes the proof by noting that $1/\sqrt{t} \sum_{k=0}^{t-1} \boldsymbol{\omega}_k = 1/\sqrt{t} \sum_{k=1}^t \boldsymbol{\omega}_k - \boldsymbol{\omega}_t/\sqrt{t} + \boldsymbol{\omega}_0/\sqrt{t}$ and $\boldsymbol{\omega}_t \rightarrow \mathbf{0}$ as $t \rightarrow 0$ almost surely.

• **Proof of (a).** By Lemma A.3, we know $\boldsymbol{\theta}_i$ is a martingale difference with the limiting covariance $\mathbb{E}[(I - \tilde{C}^*) \Xi^* (I - \tilde{C}^*)^\top]$. Thus, it suffices to verify the following Lindeberg condition.

Lemma B.1. Under the conditions of Theorem 3.5, we have for any $\epsilon > 0$, almost surely,

$$\frac{1}{t} \sum_{i=0}^{t-1} \mathbb{E} \left[\|\boldsymbol{\theta}_i\|^2 \cdot \mathbf{1}_{\|\boldsymbol{\theta}_i\| > \epsilon\sqrt{t}} \mid \mathcal{F}_{i-1} \right] \rightarrow 0 \quad \text{as } t \rightarrow \infty.$$

With the above Lindeberg condition, we apply the martingale central limit theorem in (Duflo, 2013, Proposition 2.1.9) and obtain the result in (a).

• **Proof of (b).** We need the following lemma to provide the uniform bounds for matrices B_i^t and A_i^t in (B.1).

Lemma B.2 (Adapted Lemma 1 in Polyak and Juditsky (1992)). Given $I - C^*$ is positive definite, there is a constant $\Upsilon_{AB} > 0$ such that $\max\{\|B_i^t\|, \|A_i^t\|\} \leq \Upsilon_{AB}$, $\forall i, t \geq 0$. Furthermore, we have $\lim_{t \rightarrow \infty} \frac{1}{t} \sum_{i=0}^t \|A_i^t\| = 0$.

With the above lemma and the fact that $\sup_{i \geq 0} \mathbb{E}[\|\theta_i\|^2] < \infty$ (see (C.2) in proving Lemma B.1), we have

$$\mathbb{E} \left[\left\| \frac{1}{\sqrt{t}} \sum_{i=0}^{t-1} A_i^{t-1} \theta_i \right\|^2 \right] = \frac{1}{t} \sum_{i=0}^{t-1} \mathbb{E} [\|A_i^{t-1} \theta_i\|^2] \leq \Upsilon_{AB} \cdot \left(\sup_{i \geq 0} \mathbb{E}[\|\theta_i\|^2] \right) \cdot \frac{1}{t} \sum_{i=0}^{t-1} \|A_i^{t-1}\| \rightarrow 0$$

as $t \rightarrow \infty$. Thus, $\frac{1}{\sqrt{t}} \sum_{i=0}^{t-1} A_i^{t-1} \theta_i = o_p(1)$ and this shows (b).

• **Proof of (c).** By Lemma B.2, we know it suffices to show that $1/\sqrt{t} \sum_{i=0}^{t-1} \|\delta_i\| \xrightarrow{a.s.} 0$ as $t \rightarrow \infty$. We note that

$$\begin{aligned} \|\delta_i\| &\stackrel{(A.3b)}{\leq} 2 \{ \|(K^*)^{-1}\| \cdot \|\psi_i\| + \|K_i^{-1} - (K^*)^{-1}\| \cdot \|\nabla \mathcal{L}_i\| \} + \|C_i - C^*\| \cdot \|\omega_i\| \quad (\|C_t\| \leq 1) \\ &\leq 2\Upsilon_K \Upsilon_L \|\omega_i\|^2 + 2\Upsilon_K^2 \|K_i - K^*\| \cdot \|\nabla \mathcal{L}_i\| + \frac{2\tau\Upsilon_S}{\sigma_{\min}(K^*)} \|K_i - K^*\| \cdot \|\omega_i\|, \end{aligned} \quad (\text{B.3})$$

where the second inequality is due to Assumption 3.1, Lemma A.2, and Lemma A.1(c). We present the following lemma that studies the convergence of the terms on the right hand side.

Lemma B.3. Under the conditions of Theorem 3.5, we have as $t \rightarrow \infty$,

$$\frac{1}{\sqrt{t}} \sum_{i=0}^{t-1} \|\omega_i\|^2 \xrightarrow{a.s.} 0 \quad \text{and} \quad \frac{1}{\sqrt{t}} \sum_{i=0}^{t-1} \|K_i - K^*\| \cdot (\|\omega_i\| + \|\nabla \mathcal{L}_i\|) \xrightarrow{a.s.} 0.$$

Combining Lemma B.3 with (B.3), we prove the result in (c).

• **Proof of (d).** By (11) and Lemma B.2, it suffices to show that $1/\sqrt{t} \sum_{i=0}^{t-1} \chi_i \|\mathbf{z}_{i,\tau}\|/\beta_i \xrightarrow{a.s.} 0$ as $t \rightarrow \infty$. In fact, we know

$$\mathbb{E} \left[\sum_{i=0}^{\infty} \frac{1}{\sqrt{i+1}} \frac{\chi_i}{\beta_i} \|\mathbf{z}_{i,\tau}\| \right] = \sum_{i=0}^{\infty} \frac{1}{\sqrt{i+1}} \frac{\chi_i}{\beta_i} \mathbb{E}[\|\mathbf{z}_{i,\tau}\|] \leq \frac{\Upsilon_z c_{\chi}}{c_{\beta}} \sum_{i=0}^{\infty} \frac{1}{(i+1)^{\chi-\beta+0.5}} < \infty,$$

where the last inequality is due to $\chi > \beta + 0.5$. By Kronecker's lemma in Lemma A.5, we obtain the result in (d).

• **Proof of (e).** The result in (e) is trivial due to Lemma B.2.

B.2 Proof of Proposition 3.6

By the definitions of $\bar{\Xi}^*$ in (17) and Ξ^* in (14), we have

$$\begin{aligned} \bar{\Xi}^* - \Xi^* &= (I - C^*)^{-1} \mathbb{E} \left[(I - \tilde{C}^*) \Xi^* (I - \tilde{C}^*)^\top \right] (I - C^*)^{-1} - \Xi^* \\ &= (I - C^*)^{-1} \mathbb{E}[(\tilde{C}^* - C^*) \Xi^* (\tilde{C}^* - C^*)^\top] (I - C^*)^{-1}. \end{aligned} \quad (\text{B.4})$$

(a) **Without the sketching solver.** In this case, we have $C^* = \tilde{C}^* = \mathbf{0}$, hence $\bar{\Xi}^* = \Xi^*$.

(b) With the sketching solver. Since $\Xi^* \succeq 0$, we know $(I - C^*)^{-1} \mathbb{E}[(\tilde{C}^* - C^*)\Xi^*(\tilde{C}^* - C^*)^\top](I - C^*)^{-1} \succeq 0$, then we have $\bar{\Xi}^* \succeq \Xi^*$ by (B.4). Next, we recall that $\rho = 1 - \gamma_S$ and have that

$$\begin{aligned} \|\bar{\Xi}^* - \Xi^*\| &\stackrel{(B.4)}{=} \|(I - C^*)^{-1} \mathbb{E}[(\tilde{C}^* - C^*)\Xi^*(\tilde{C}^* - C^*)^\top](I - C^*)^{-1}\| \\ &\leq \|(I - C^*)^{-1}\|^2 \cdot \|\mathbb{E}[(\tilde{C}^* - C^*)\Xi^*(\tilde{C}^* - C^*)^\top]\| \\ &\leq \frac{1}{(1 - \rho^\tau)^2} \cdot \|\mathbb{E}[\tilde{C}^* \Xi^* (\tilde{C}^*)^\top] - C^* \Xi^* C^*\| \\ &\leq \frac{1}{(1 - \rho^\tau)^2} \cdot \left(\|\mathbb{E}[\tilde{C}^* \Xi^* (\tilde{C}^*)^\top]\| + \rho^{2\tau} \|\Xi^*\| \right), \end{aligned} \quad (B.5)$$

where the third and fourth inequalities use $\|C^*\| \leq \rho^\tau$ in Lemma A.1(a) and Lemma A.2(a). Furthermore, we have

$$\begin{aligned} \mathbf{0} &\preceq \mathbb{E}[\tilde{C}^* \Xi^* (\tilde{C}^*)^\top] \preceq \|\Xi^*\| \cdot \mathbb{E}[\tilde{C}^* (\tilde{C}^*)^\top] \\ &\stackrel{(15)}{=} \|\Xi^*\| \cdot \mathbb{E} \left[\left(\prod_{j=1}^{\tau} (I - K^* S_j (S_j^\top (K^*)^2 S_j)^\dagger S_j^\top K^*) \right) \left(\prod_{j=1}^{\tau} (I - K^* S_j (S_j^\top (K^*)^2 S_j)^\dagger S_j^\top K^*)^\top \right) \right] \\ &= \|\Xi^*\| \cdot \mathbb{E} \left[\left(\prod_{j=2}^{\tau} (I - K^* S_j (S_j^\top (K^*)^2 S_j)^\dagger S_j^\top K^*) \right) \mathbb{E}[(I - K^* S_1 (S_1^\top (K^*)^2 S_1)^\dagger S_1^\top K^*) | S_2, S_3, \dots, S_\tau] \right. \\ &\quad \left. \left(\prod_{j=2}^{\tau} (I - K^* S_j (S_j^\top (K^*)^2 S_j)^\dagger S_j^\top K^*)^\top \right) \right] \\ &\preceq \|\Xi^*\| \cdot \rho \cdot \mathbb{E} \left[\left(\prod_{j=2}^{\tau} (I - K^* S_j (S_j^\top (K^*)^2 S_j)^\dagger S_j^\top K^*) \right) \left(\prod_{j=2}^{\tau} (I - K^* S_j (S_j^\top (K^*)^2 S_j)^\dagger S_j^\top K^*)^\top \right) \right], \end{aligned} \quad (B.6)$$

where the fourth equality uses the fact that $(I - K^* S_j (S_j^\top (K^*)^2 S_j)^\dagger S_j^\top K^*)$ is a projection matrix for all $j \in [1, \tau]$, and the last inequality uses Assumption 3.3 and $K_t \rightarrow K^*$ in Lemma A.2. We then repeat (B.6) for τ times, and finally get that

$$\mathbf{0} \preceq \mathbb{E}[\tilde{C}^* \Xi^* (\tilde{C}^*)^\top] \preceq \rho^\tau \|\Xi^*\| \cdot I. \quad (B.7)$$

Then, we combine (B.7) with (B.5), and obtain that

$$\|\bar{\Xi}^* - \Xi^*\| \leq \frac{(\rho^\tau + \rho^{2\tau})}{(1 - \rho^\tau)^2} \cdot \|\Xi^*\| \leq \frac{(1 + \rho^\tau)}{(1 - \rho^\tau)^2} \rho^\tau \cdot \|\Xi^*\|.$$

This completes the proof.

B.3 Proof of Proposition 3.7

With $c_\beta = 1$ and $\beta = 1$, the Lyapunov equation (19) can be written as

$$(0.5I - C^*)\tilde{\Xi}^* + \tilde{\Xi}^*(0.5I - C^*) = \mathbb{E}[(I - \tilde{C}^*)\Xi^*(I - \tilde{C}^*)^\top].$$

Recall from (17) that $\bar{\Xi}^* = (I - C^*)^{-1} \mathbb{E}[(I - \tilde{C}^*) \Xi^* (I - \tilde{C}^*)^\top] (I - C^*)^{-1}$, then we obtain

$$\begin{aligned}
(0.5I - C^*) &(\tilde{\Xi}^* - \bar{\Xi}^*) + (\tilde{\Xi}^* - \bar{\Xi}^*)(0.5I - C^*) \\
&= \mathbb{E}[(I - \tilde{C}^*) \Xi^* (I - \tilde{C}^*)^\top] - \bar{\Xi}^* + C^* \bar{\Xi}^* + \bar{\Xi}^* C^* \\
&= \mathbb{E}[(I - \tilde{C}^*) \Xi^* (I - \tilde{C}^*)^\top] - (I - C^*) \bar{\Xi}^* - \bar{\Xi}^* (I - C^*) + \bar{\Xi}^* \\
&= (I - (I - C^*)^{-1}) \mathbb{E}[(I - \tilde{C}^*) \Xi^* (I - \tilde{C}^*)^\top] (I - (I - C^*)^{-1}) \\
&\succeq \mathbf{0}.
\end{aligned}$$

By Lemma A.1, we have $\|C^*\| \leq \rho^\tau < 1/2$, then the basic Lyapunov theorem (Khalil, 2002, Theorem 4.6) suggests that $\tilde{\Xi}^* \succeq \bar{\Xi}^*$. This completes the proof.

B.4 Proof of Theorem 4.1

Recall that $\omega_k = (\mathbf{x}_k - \mathbf{x}^*, \boldsymbol{\lambda}_k - \boldsymbol{\lambda}^*)$. Following the same decomposition in (B.2), the partial sum process can be decomposed as

$$\begin{aligned}
\frac{1}{\sqrt{t}} \sum_{k=1}^{\lfloor rt \rfloor} \omega_k &\stackrel{(B.2)}{=} \frac{1}{\sqrt{t}} \sum_{i=0}^{\lfloor rt \rfloor - 1} (I - C^*)^{-1} \boldsymbol{\theta}_i + \frac{1}{\sqrt{t}} \sum_{i=0}^{\lfloor rt \rfloor - 1} A_i^{\lfloor rt \rfloor - 1} \boldsymbol{\theta}_i + \frac{1}{\sqrt{t}} \sum_{i=0}^{\lfloor rt \rfloor - 1} B_i^{\lfloor rt \rfloor - 1} \left(\boldsymbol{\delta}_i + \frac{\bar{\alpha}_i - \beta_i}{\beta_i} \mathbf{z}_{i,\tau} \right) \\
&\quad + \frac{1}{\sqrt{t} \beta_0} B_0^{\lfloor rt \rfloor - 1} [I - \beta_0(I - C^*)] \omega_0 \\
&= \frac{1}{\sqrt{t}} \sum_{i=0}^{\lfloor rt \rfloor - 1} (I - C^*)^{-1} \boldsymbol{\theta}_i + \frac{1}{\sqrt{t}} \sum_{i=0}^{\lfloor rt \rfloor - 1} A_i^{t-1} \boldsymbol{\theta}_i + \frac{1}{\sqrt{t}} \sum_{i=0}^{\lfloor rt \rfloor - 1} (A_i^{\lfloor rt \rfloor - 1} - A_i^{t-1}) \boldsymbol{\theta}_i \\
&\quad + \frac{1}{\sqrt{t}} \sum_{i=0}^{\lfloor rt \rfloor - 1} B_i^{\lfloor rt \rfloor - 1} \left(\boldsymbol{\delta}_i + \frac{\bar{\alpha}_i - \beta_i}{\beta_i} \mathbf{z}_{i,\tau} \right) + \frac{1}{\sqrt{t} \beta_0} B_0^{\lfloor rt \rfloor - 1} [I - \beta_0(I - C^*)] \omega_0,
\end{aligned}$$

where $r \in [0, 1]$, and $A_i^{\lfloor rt \rfloor}$ and $B_i^{\lfloor rt \rfloor}$ are defined in (B.1). In what follows, we analyze each right-hand-side term above and establish the following claims:

- (a): $\frac{1}{\sqrt{t}} \sum_{i=0}^{\lfloor rt \rfloor - 1} (I - C^*)^{-1} \boldsymbol{\theta}_i \implies (\bar{\Xi}^*)^{1/2} W_{d+m}(r)$, where $\bar{\Xi}^*$ is defined in (17).
- (b): $\sup_{r \in [0, 1]} \left\| \frac{1}{\sqrt{t}} \sum_{i=0}^{\lfloor rt \rfloor - 1} A_i^{t-1} \boldsymbol{\theta}_i \right\| = o_p(1)$.
- (c): $\sup_{r \in [0, 1]} \left\| \frac{1}{\sqrt{t}} \sum_{i=0}^{\lfloor rt \rfloor - 1} (A_i^{\lfloor rt \rfloor - 1} - A_i^{t-1}) \boldsymbol{\theta}_i \right\| = o_p(1)$.
- (d): $\sup_{r \in [0, 1]} \left\| \frac{1}{\sqrt{t}} \sum_{i=0}^{\lfloor rt \rfloor - 1} B_i^{\lfloor rt \rfloor - 1} \boldsymbol{\delta}_i \right\| = o(1)$.
- (e): $\sup_{r \in [0, 1]} \left\| \frac{1}{\sqrt{t}} \sum_{i=0}^{\lfloor rt \rfloor - 1} B_i^{\lfloor rt \rfloor - 1} \frac{(\bar{\alpha}_i - \beta_i)}{\beta_i} \mathbf{z}_{i,\tau} \right\| = o(1)$.
- (f): $\sup_{r \in [0, 1]} \left\| \frac{1}{\sqrt{t} \beta_0} B_0^{\lfloor rt \rfloor - 1} (I - \beta_0(I - C^*)) \omega_0 \right\| = o(1)$.

Combining these claims together, we obtain

$$\frac{1}{\sqrt{t}} \sum_{k=1}^{\lfloor rt \rfloor} \omega_k \implies (\bar{\Xi}^*)^{1/2} W_{d+m}(r).$$

This completes the proof of the theorem by noting that $\frac{1}{\sqrt{t}} \sum_{k=0}^{\lfloor rt \rfloor - 1} \omega_k = \frac{1}{\sqrt{t}} \sum_{k=1}^{\lfloor rt \rfloor} \omega_k - \frac{1}{\sqrt{t}} \omega_{\lfloor rt \rfloor} + \frac{1}{\sqrt{t}} \omega_0$ and the fact that $\sup_{r \in [0, 1]} \|\omega_{\lfloor rt \rfloor}\| / \sqrt{t} = o(1)$.

- **Proof of (a).** By Lemma A.3, we know that $\boldsymbol{\theta}_i$ is a martingale difference and the conditional covariance of $\boldsymbol{\theta}_i$ converges almost surely to $\mathbb{E}[(I - \tilde{C}^*)\Xi^*(I - \tilde{C}^*)^\top]$. By Lemma B.1, we have verified the Lindeberg condition. Then, we apply the martingale Functional Central Limit Theorem (FCLT) (Hall and Heyde, 2014, Theorem 4.2), we have as $t \rightarrow \infty$

$$\frac{1}{\sqrt{t}} \sum_{i=0}^{\lfloor rt \rfloor - 1} (I - C^*)^{-1} \boldsymbol{\theta}_i \xrightarrow{\text{D}} (\bar{\Xi}^*)^{1/2} W_{d+m}(r).$$

This completes the proof of (a).

- **Proof of (b).** Note that $\sum_{i=0}^{\lfloor rt \rfloor - 1} A_i^{t-1} \boldsymbol{\theta}_i$ is a martingale indexed by $r \in [0, 1]$. By Doob's inequality (Hall and Heyde, 2014, Theorem 2.2), we have

$$\begin{aligned} \mathbb{E} \left[\sup_{r \in [0, 1]} \left\| \frac{1}{\sqrt{t}} \sum_{i=0}^{\lfloor rt \rfloor - 1} A_i^{t-1} \boldsymbol{\theta}_i \right\|^2 \right] &\leq \frac{4}{t} \mathbb{E} \left[\left\| \sum_{i=0}^{t-1} A_i^{t-1} \boldsymbol{\theta}_i \right\|^2 \right] = \frac{4}{t} \sum_{i=0}^{t-1} \mathbb{E} \left[\|A_i^{t-1} \boldsymbol{\theta}_i\|^2 \right] \\ &\leq \Upsilon_{AB} \cdot \left(\sup_{i \geq 0} \mathbb{E}[\|\boldsymbol{\theta}_i\|^2] \right) \cdot \frac{4}{t} \sum_{i=0}^{t-1} \|A_i^{t-1}\| \rightarrow 0, \end{aligned}$$

where the last inequality is due to Lemma B.2 and the fact that $\boldsymbol{\theta}_i$ has bounded $(2 + \delta)$ -moment (see (C.2) in proving Lemma B.1). Thus, we have $\sup_{r \in [0, 1]} \left\| \frac{1}{\sqrt{t}} \sum_{i=0}^{\lfloor rt \rfloor - 1} A_i^{t-1} \boldsymbol{\theta}_i \right\| = o_p(1)$ and complete the proof of (b).

- **Proof of (c).** We notice that for any integer $n \in \{0, 1, 2, \dots, t-1\}$,

$$\begin{aligned} \sum_{i=0}^n (A_i^{t-1} - A_i^n) \boldsymbol{\theta}_i &\stackrel{(B.1)}{=} \sum_{i=0}^n (B_i^{t-1} - B_i^n) \boldsymbol{\theta}_i \stackrel{(B.1)}{=} \sum_{i=0}^n \sum_{k=n+1}^{t-1} \prod_{j=i+1}^k (I - \beta_j(I - C^*)) \beta_i \boldsymbol{\theta}_i \\ &= \sum_{k=n+1}^{t-1} \sum_{i=0}^n \prod_{j=i+1}^k (I - \beta_j(I - C^*)) \beta_i \boldsymbol{\theta}_i \\ &= \frac{1}{\beta_{n+1}} \cdot \beta_{n+1} \sum_{k=n+1}^{t-1} \prod_{j=n+1}^k (I - \beta_j(I - C^*)) \left[\sum_{i=0}^n \prod_{j=i+1}^n (I - \beta_j(I - C^*)) \beta_i \boldsymbol{\theta}_i \right] \\ &\stackrel{(B.1)}{=} \frac{1}{\beta_{n+1}} \cdot B_{n+1}^{t-1} (I - \beta_{n+1}(I - C^*)) \left[\sum_{i=0}^n \prod_{j=i+1}^n (I - \beta_j(I - C^*)) \beta_i \boldsymbol{\theta}_i \right]. \quad (\text{B.8}) \end{aligned}$$

By Lemma B.2, we know that $\|B_{n+1}^{t-1} (I - \beta_{n+1}(I - C^*))\| \leq \Upsilon_{AB} (1 + 2c_\beta)$ for any $n, t \geq 0$. Thus, we obtain

$$\begin{aligned} \sup_{r \in [0, 1]} \left\| \frac{1}{\sqrt{t}} \sum_{i=0}^{\lfloor rt \rfloor - 1} (A_i^{\lfloor rt \rfloor - 1} - A_i^{t-1}) \boldsymbol{\theta}_i \right\| &= \sup_{n \in [0, t-1]} \left\| \frac{1}{\sqrt{t}} \sum_{i=0}^n (A_i^n - A_i^{t-1}) \boldsymbol{\theta}_i \right\| \\ &\stackrel{(B.8)}{\leq} \Upsilon_{AB} (1 + 2c_\beta) \sup_{n \in [0, t-1]} \left\| \frac{1}{\sqrt{t}} \frac{1}{\beta_{n+1}} \sum_{i=0}^n \prod_{j=i+1}^n (I - \beta_j(I - C^*)) \beta_i \boldsymbol{\theta}_i \right\|. \quad (\text{B.9}) \end{aligned}$$

We need a technical lemma to proceed with the proof.

Lemma B.4 (Adapted Lemma B.2 in [Li et al. \(2023\)](#)). Let $\{\boldsymbol{\theta}_n\}_{n \geq 0}$ be a martingale difference sequence. Given the matrix $I - C^*$ is positive definite, we define an auxiliary sequence $\{\mathbf{y}_n\}_{n \geq 0}$ as follows: $\mathbf{y}_0 = \mathbf{0}$, and for $n \geq 0$,

$$\mathbf{y}_{n+1} = \sum_{i=0}^n \left(\prod_{j=i+1}^n (I - \beta_j(I - C^*)) \right) \beta_i \boldsymbol{\theta}_i.$$

Let the step size $\beta_i = c_\beta/(i+1)^\beta$ for some $c_\beta > 0$ and $\beta \in (0.5, 1)$. If $\sup_{i \geq 0} \mathbb{E} \|\boldsymbol{\theta}_i\|^{2+\delta} < \infty$ for some $\delta > 0$, then we have that as $t \rightarrow \infty$,

$$\sup_{n \in [0, t-1]} \left\| \frac{1}{\sqrt{t}} \frac{1}{\beta_{n+1}} \sum_{i=0}^n \prod_{j=i+1}^n (I - \beta_j(I - C^*)) \beta_i \boldsymbol{\theta}_i \right\| = o_p(1).$$

We recall that $\boldsymbol{\theta}_i$ is a martingale difference with $(2 + \delta)$ -th bounded moment [\(C.2\)](#). Thus, we directly apply Lemma B.4 to [\(B.9\)](#) and complete the proof of [\(c\)](#).

• **Proof of (d).** By Lemma B.2, we know that $\|B_i^t\| \leq \Upsilon_{AB}$ for any $i, t \geq 0$, then as $t \rightarrow \infty$,

$$\sup_{r \in [0, 1]} \left\| \frac{1}{\sqrt{t}} \sum_{i=0}^{\lfloor rt \rfloor - 1} B_i^{\lfloor rn \rfloor - 1} \boldsymbol{\delta}_i \right\| \leq \frac{\Upsilon_{AB}}{\sqrt{t}} \sum_{i=0}^{t-1} \|\boldsymbol{\delta}_i\| \xrightarrow{a.s.} 0,$$

where the convergence holds due to [\(B.3\)](#) and Lemma B.3. This completes the proof of [\(d\)](#).

• **Proof of (e).** By Lemma B.2, we know that $\|B_i^t\| \leq \Upsilon_{AB}$ for any $i, t \geq 0$, then as $t \rightarrow \infty$,

$$\sup_{r \in [0, 1]} \left\| \frac{1}{\sqrt{t}} \sum_{i=0}^{\lfloor rt \rfloor - 1} B_i^{\lfloor rt \rfloor - 1} \frac{(\bar{\alpha}_i - \beta_i)}{\beta_i} \mathbf{z}_{i, \tau} \right\| \leq \frac{\Upsilon_{AB}}{\sqrt{t}} \sum_{i=0}^{t-1} \frac{\chi_i}{\beta_i} \|\mathbf{z}_{i, \tau}\| \xrightarrow{a.s.} 0.$$

where the convergence holds due to the proof of [\(d\)](#) in Section B.1. This completes the proof of [\(e\)](#).

• **Proof of (f).** By Lemma B.2, we know that $\|B_i^t\| \leq \Upsilon_{AB}$ for any $i, t \geq 0$, then as $t \rightarrow \infty$,

$$\sup_{r \in [0, 1]} \left\| \frac{1}{\sqrt{t} \beta_0} B_0^{\lfloor rt \rfloor} (I - \beta_0(I - C^*)) \boldsymbol{\omega}_0 \right\| \leq \frac{\Upsilon_{AB}}{\sqrt{t} \beta_0} \|(I - \beta_0(I - C^*)) \boldsymbol{\omega}_0\| \rightarrow 0.$$

This completes the proof of [\(f\)](#).

B.5 Proof of Theorem 4.2

We first state the following Lemma, which shows that the vector $\mathbf{w} \in \mathbb{R}^{d+m}$ defined in Theorem 4.2 satisfies $\mathbf{w}^\top \bar{\Xi}^* \mathbf{w} > 0$, where $\bar{\Xi}^*$ is defined in [\(17\)](#).

Lemma B.5. Let $G^* = \nabla c(\mathbf{x}^*)$ be the constraint Jacobian evaluated at \mathbf{x}^* . Suppose $\text{cov}(\nabla F(\mathbf{x}^*; \xi)) \succ 0$, for any vector $\mathbf{w} = (\mathbf{w}_x, \mathbf{w}_\lambda) \in \mathbb{R}^{d+m}$ with $\mathbf{w} \notin \text{Span}((G^*)^\top) \otimes \mathbf{0}_m$, we have $\mathbf{w}^\top \bar{\Xi}^* \mathbf{w} > 0$.

Recall the definition that $\boldsymbol{\omega}_t = (\mathbf{x}_t - \mathbf{x}^*, \boldsymbol{\lambda}_t - \boldsymbol{\lambda}^*)$, we consider the following random function

$$C_t(r) := \frac{1}{\sqrt{t}} \sum_{i=0}^{\lfloor rt \rfloor - 1} \mathbf{w}^\top \boldsymbol{\omega}_i.$$

Based on Theorem 4.1, the one-dimensional random function $C_t(r)$ satisfies:

$$C_t(r) \implies (\mathbf{w}^\top \bar{\Xi}^* \mathbf{w})^{1/2} W_1(r), \quad r \in [0, 1],$$

where $W_1(\cdot)$ stands for the standard one-dimensional Brownian motion. Define $\bar{\omega}_t = \frac{1}{t} \sum_{i=0}^{t-1} \omega_i$. Then, we have

$$\begin{aligned} \frac{\sqrt{t} \mathbf{w}^\top \bar{\omega}_t}{\sqrt{\mathbf{w}^\top V_t \mathbf{w}}} &= \frac{C_t(1)}{\sqrt{\frac{1}{t} \sum_{i=1}^t \left\{ \frac{i}{\sqrt{t}} \mathbf{w}^\top (\bar{\omega}_i - \bar{\omega}_t) \right\}^2}} \\ &= \frac{C_t(1)}{\sqrt{\frac{1}{t} \sum_{i=1}^t \left\{ \frac{i}{\sqrt{t}} \mathbf{w}^\top \left[\frac{1}{i} \sum_{k=0}^{i-1} \omega_k - \frac{1}{t} \sum_{k=0}^{t-1} \omega_k \right] \right\}^2}} = \frac{C_t(1)}{\sqrt{\frac{1}{t} \sum_{i=1}^t \left\{ C_t \left(\frac{i}{t} \right) - \frac{i}{t} C_t(1) \right\}^2}}. \end{aligned}$$

By the Riemann integral approximation, as $t \rightarrow \infty$, we have

$$\frac{1}{t} \sum_{i=1}^t \left(C_t \left(\frac{i}{t} \right) - \frac{i}{t} C_t(1) \right)^2 \rightarrow \int_0^1 (C_t(r) - r C_t(1))^2 dr.$$

Since $\frac{C_t(1)}{\sqrt{\int_0^1 (C_t(r) - r C_t(1))^2 dr}}$ is a continuous functional of $C_t(\cdot)$, the continuous mapping theorem (Whitt, 2002, Theorem 3.4.3) implies

$$\begin{aligned} \frac{C_t(1)}{\sqrt{\frac{1}{t} \sum_{i=1}^t \left(C_t \left(\frac{i}{t} \right) - \frac{i}{t} C_t(1) \right)^2}} &\xrightarrow{d} \frac{(\mathbf{w}^\top \bar{\Xi}^* \mathbf{w})^{1/2} \cdot W_1(1)}{(\mathbf{w}^\top \bar{\Xi}^* \mathbf{w})^{1/2} \cdot \sqrt{\int_0^1 (W_1(r) - r W_1(1))^2 dr}} \\ &= \frac{W_1(1)}{\sqrt{\int_0^1 (W_1(r) - r W_1(1))^2 dr}}, \end{aligned}$$

where the last equality follows since $\mathbf{w}^\top \bar{\Xi}^* \mathbf{w} > 0$ by Lemma B.5. Therefore, we obtain

$$\frac{\sqrt{t} \mathbf{w}^\top \bar{\omega}_t}{\sqrt{\mathbf{w}^\top V_t \mathbf{w}}} \xrightarrow{d} \frac{W_1(1)}{\sqrt{\int_0^1 (W_1(r) - r W_1(1))^2 dr}},$$

which completes the proof.

C Proofs of Technical Lemmas

C.1 Proof of Lemma B.1

By Assumption 3.1, there exists a constant $\Upsilon_u > 0$ such that

$$\|\nabla^2 \mathcal{L}(\mathbf{x}, \boldsymbol{\lambda})\| \vee \|\nabla \mathcal{L}(\mathbf{x}, \boldsymbol{\lambda})\| \leq \Upsilon_u, \quad \forall (\mathbf{x}, \boldsymbol{\lambda}) \in \mathcal{X} \times \Lambda. \quad (\text{C.1})$$

For $\delta > 0$ in Assumption 3.2, we let $q = 2 + \delta$ and have

$$\begin{aligned}
\mathbb{E}[\|\boldsymbol{\theta}_i\|^q \mid \mathcal{F}_{i-1}] &\stackrel{(A.3a)}{\leq} 2^{q-1} \{ \mathbb{E}[\|(I - C_i)K_i^{-1}(\bar{\nabla}\mathcal{L}_i - \nabla\mathcal{L}_i)\|^q \mid \mathcal{F}_{i-1}] + \mathbb{E}[\|\boldsymbol{z}_{i,\tau} - (I - C_i)\tilde{\boldsymbol{z}}_i\|^q \mid \mathcal{F}_{i-1}] \} \\
&\stackrel{(A.2)}{\leq} 2^{q-1} \left(\mathbb{E}[\|(I - C_i)K_i^{-1}\|^q \|\bar{g}_i - \nabla f_i\|^q \mid \mathcal{F}_{i-1}] + \mathbb{E}[\|(\tilde{C}_i - C_i)\tilde{\boldsymbol{z}}_i\|^q \mid \mathcal{F}_{i-1}] \right) \\
&\leq 2^{q-1} (2^q \Upsilon_K^p \mathbb{E}[\|\bar{g}_i - \nabla f_i\|^q \mid \mathcal{F}_{i-1}] + 2^q \mathbb{E}[\|\tilde{\boldsymbol{z}}_i\|^q \mid \mathcal{F}_{i-1}]) \quad (\|\tilde{C}_i\| \leq 1, \|C_i\| \leq 1, \|K_i^{-1}\| \leq \Upsilon_K) \\
&\stackrel{(12)}{\leq} 2^{q-1} (2^q \Upsilon_K^q \Upsilon_m + 2^q \mathbb{E}[\|\tilde{\boldsymbol{z}}_i\|^q \mid \mathcal{F}_{i-1}]) \\
&\stackrel{(6)}{\leq} 2^{q-1} (2^q \Upsilon_K^q \Upsilon_m + 2^q \Upsilon_K^q \mathbb{E}[\|\bar{\nabla}\mathcal{L}_i\|^q \mid \mathcal{F}_{i-1}]) \quad (\|K_i^{-1}\| \leq \Upsilon_K) \\
&\leq 2^{q-1} (2^q \Upsilon_K^q \Upsilon_m + 2^q \Upsilon_K^q \{2^{q-1} \|\nabla\mathcal{L}_i\|^q + 2^{q-1} \mathbb{E}[\|\bar{g}_i - \nabla f_i\|^q \mid \mathcal{F}_{i-1}]\}) \\
&\stackrel{(12)}{\leq} 2^{q-1} (2^q \Upsilon_K^q \Upsilon_m + 2^q \Upsilon_K^q \{2^{q-1} \Upsilon_u^q + 2^{q-1} \Upsilon_m\}) =: C_q, \tag{C.2}
\end{aligned}$$

where the first inequality is due to Jensen's inequality; $\|K_i^{-1}\| \leq \Upsilon_K$ is due to Lemma A.2(b); and the last inequality is also due to (C.1). With the above display, we have for any $\epsilon > 0$,

$$\frac{1}{t} \sum_{i=0}^{t-1} \mathbb{E} \left[\|\boldsymbol{\theta}_i\|^2 \cdot \mathbf{1}_{\|\boldsymbol{\theta}_i\| > \epsilon \sqrt{t}} \mid \mathcal{F}_{i-1} \right] \leq \frac{1}{\epsilon^\delta t^{1+\delta/2}} \sum_{i=0}^{t-1} \mathbb{E} \left[\|\boldsymbol{\theta}_i\|^{2+\delta} \mid \mathcal{F}_{i-1} \right] \leq \frac{C_{2+\delta}}{\epsilon^\delta t^{\delta/2}} \longrightarrow 0.$$

This completes the proof.

C.2 Proof of Lemma B.3

By (C.1), we have $\|\nabla\mathcal{L}_i\| \leq \Upsilon_u \|\boldsymbol{\omega}_i\|$. By the fact $\|K_i - K^*\| \|\boldsymbol{\omega}_i\| \leq 0.5(\|K_i - K^*\|^2 + \|\boldsymbol{\omega}_i\|^2)$, we know it suffices to show $1/\sqrt{t} \cdot \sum_{i=0}^{t-1} (\|\boldsymbol{\omega}_i\|^2 + \|K_i - K^*\|^2) \rightarrow 0$ as $t \rightarrow \infty$ almost surely. Note that

$$\begin{aligned}
\|K_i - K^*\| &\stackrel{(6),(14)}{=} \left\| \begin{pmatrix} B_i - \nabla_x^2 \mathcal{L}^* & G_i^\top - (G^*)^\top \\ G_i - G^* & 0 \end{pmatrix} \right\| \\
&\leq \left\| \begin{pmatrix} \frac{1}{i} \sum_{j=0}^{i-1} \bar{\nabla}_x^2 \mathcal{L}_j - \nabla_x^2 \mathcal{L}^* & G_i^\top - (G^*)^\top \\ G_i - G^* & 0 \end{pmatrix} \right\| + \|\Delta_i\| \\
&\leq \left\| \frac{1}{i} \sum_{j=0}^{i-1} \bar{\nabla}_x^2 \mathcal{L}_j - \nabla_x^2 \mathcal{L}^* \right\| + \|G_i - G^*\| + \|\Delta_i\| \\
&\leq \left\| \frac{1}{i} \sum_{j=0}^{i-1} (\bar{H}_j - \nabla^2 f_j) \right\| + \frac{1}{i} \sum_{j=0}^{i-1} \|\nabla_x^2 \mathcal{L}_j - \nabla_x^2 \mathcal{L}^*\| + \|G_i - G^*\| + \|\Delta_i\| \\
&\leq \left\| \frac{1}{i} \sum_{j=0}^{i-1} (\bar{H}_j - \nabla^2 f_j) \right\| + \frac{\Upsilon_L}{i} \sum_{j=0}^{i-1} \|\boldsymbol{\omega}_j\| + \Upsilon_L \|\boldsymbol{\omega}_i\| + \|\Delta_i\| \quad (\text{Assumption 3.1}). \tag{C.3}
\end{aligned}$$

By Lemma A.2(a), the regularization term $\Delta_i = 0$ for all sufficiently large i almost surely. Thus, we focus on the first two terms on the right hand side. Let us define

$$R_i := \left\| \frac{1}{i} \sum_{j=0}^{i-1} (\bar{H}_j - \nabla^2 f_j) \right\| + \frac{1}{i} \sum_{j=0}^{i-1} \|\boldsymbol{\omega}_j\| \quad \text{for } i \geq 0, \tag{C.4}$$

and for any fixed integer $t_0 > 0$ and a constant $\nu > 0$, we define a stopping time

$$\mu_{t_0, \nu} = \inf\{t \geq t_0 : \|K_t - K^*\| > \nu \text{ OR } \|\omega_t\| > \nu\}. \quad (\text{C.5})$$

The next lemma provides the convergence rate of $\|\omega_i\|^2$ and $\|R_i\|^2$ for i large enough.

Lemma C.1. Under the conditions of Theorem 3.5 and supposing

$$\nu \leq \frac{1 - \rho^\tau}{4\Upsilon_K(1 + \Upsilon_L)} \quad (\text{C.6})$$

with Υ_K from Lemma A.2(b) and Υ_L from Assumption 3.1, there exists a constant $\Upsilon_\mu > 0$ such that

$$\mathbb{E}[\|\omega_i\|^2 \mathbf{1}_{\{\mu_{t_0, \nu} > i\}}] \leq \Upsilon_\mu \beta_i \quad \text{and} \quad \mathbb{E}[R_i^2 \mathbf{1}_{\{\mu_{t_0, \nu} > i\}}] \leq \Upsilon_\mu \beta_i, \quad \forall i \geq 0.$$

By Lemma C.1, we let ν satisfy (C.6) and then obtain

$$\mathbb{E}\left[\sum_{i=0}^{\infty} \frac{1}{\sqrt{i+1}} \|\omega_i\|^2 \mathbf{1}_{\{\mu_{t_0, \nu} > i\}}\right] = \sum_{i=0}^{\infty} \frac{1}{\sqrt{i+1}} \mathbb{E}[\|\omega_i\|^2 \mathbf{1}_{\{\mu_{t_0, \nu} > i\}}] \leq \sum_{i=0}^{\infty} \frac{\Upsilon_\mu \beta_i}{\sqrt{i+1}} < \infty,$$

where the last inequality is due to $\beta_i = c_\beta/(i+1)^\beta$ with $\beta \in (0.5, 1)$. This suggests that

$$\sum_{i=0}^{\infty} \frac{1}{\sqrt{i+1}} \|\omega_i\|^2 \mathbf{1}_{\{\mu_{t_0, \nu} > i\}} < \infty \quad \text{almost surely.}$$

Since $\omega_i \rightarrow \mathbf{0}$ and $K_i \rightarrow K^*$ as $i \rightarrow \infty$ almost surely, for any run and for any $\nu > 0$, there exists t_0 such that $\mu_{t_0, \nu} = \infty$, which implies that $\sum_{i=0}^{\infty} \|\omega_i\|^2 / \sqrt{i+1} < \infty$ almost surely. By Lemma A.5, we have $\sum_{i=0}^{t-1} \|\omega_i\|^2 / \sqrt{t} \rightarrow 0$ as $t \rightarrow \infty$ almost surely. Following the same reasoning from Lemma C.1, we also obtain $\sum_{i=0}^{t-1} \|R_i\|^2 / \sqrt{t} \rightarrow 0$, implying that $\sum_{i=0}^{t-1} \|K_i - K^*\|^2 / \sqrt{t} \rightarrow 0$ as $t \rightarrow \infty$ due to (C.3) and (C.4). This completes the proof.

C.3 Proof of Lemma B.5

By Proposition 3.6, $\bar{\Xi}^* \succeq \Xi^*$. Thus, it suffices to prove $\mathbf{w}^\top \Xi^* \mathbf{w} > 0$. We recall the definition of Ξ^* in (14) and define a subspace of \mathbb{R}^{d+m} as $U := \{(\mathbf{0}, \mathbf{u}) \in \mathbb{R}^{d+m} \mid \mathbf{u} \in \mathbb{R}^m\}$. Since $\text{cov}(\nabla F(\mathbf{x}^*; \xi)) \succ 0$, we have $\mathbf{z} \in U \iff \mathbf{z}^\top \text{cov}(\nabla \mathcal{L}(\mathbf{x}^*, \boldsymbol{\lambda}^*; \xi)) \mathbf{z} = 0$. Therefore, we define two more subspaces:

$$\begin{aligned} U_1 &:= K^* U = \left\{ \begin{pmatrix} \nabla_{\mathbf{x}}^2 \mathcal{L}^* & (G^*)^\top \\ G^* & \mathbf{0} \end{pmatrix} \begin{pmatrix} \mathbf{0} \\ \mathbf{u} \end{pmatrix} \mid \mathbf{u} \in \mathbb{R}^m \right\} = \left\{ \begin{pmatrix} (G^*)^\top \mathbf{u} \\ \mathbf{0} \end{pmatrix} \mid \mathbf{u} \in \mathbb{R}^m \right\}, \\ W_1 &:= \left\{ \begin{pmatrix} \mathbf{u} \\ \mathbf{v} \end{pmatrix} \mid \mathbf{u} \in \text{Kernel}(G^*), \mathbf{v} \in \mathbb{R}^m \right\}. \end{aligned}$$

We have the direct sum decomposition $\mathbb{R}^{d+m} = U_1 \oplus W_1$. Furthermore, for any $\mathbf{z} \in U_1$, there exists a vector $\mathbf{u} \in \mathbb{R}^m$ such that

$$\mathbf{z}^\top \Xi^* \mathbf{z} = (\mathbf{0} \quad \mathbf{u}) \text{cov}(\nabla \mathcal{L}(\mathbf{x}^*, \boldsymbol{\lambda}^*; \xi)) \begin{pmatrix} \mathbf{0} \\ \mathbf{u} \end{pmatrix} = 0.$$

Conversely, if $\mathbf{z}^\top \Xi^* \mathbf{z} = 0$ for some vector $\mathbf{z} \in \mathbb{R}^{d+m}$, since K^* is invertible, there must exist a vector $\mathbf{v} \in \mathbb{R}^{d+m}$ such that $\mathbf{z} = K^* \mathbf{v}$. Thus, $\mathbf{z}^\top \Xi^* \mathbf{z} = \mathbf{v}^\top \text{cov}(\nabla \mathcal{L}(\mathbf{x}^*, \boldsymbol{\lambda}^*; \xi)) \mathbf{v} = 0$. This indicates that $\mathbf{v} \in U$ and $\mathbf{z} \in U_1$. Thus, we obtain that $\mathbf{z}^\top \Xi^* \mathbf{z} = 0 \iff \mathbf{z} \in U_1$. We complete the proof.

C.4 Proof of Lemma C.1

We first establish the convergence rate of ω_t . From (A.5) in the proof of Lemma A.3, we know

$$\omega_{t+1} = \omega_t - \beta_t(I - C_t)K_t^{-1}\nabla\mathcal{L}_t + \beta_t\theta_t + (\bar{\alpha}_t - \beta_t)\mathbf{z}_{t,\tau}. \quad (\text{C.7})$$

Given $t_0, \nu > 0$, we denote for notational brevity μ_t as the \mathcal{F}_{t-1} -measurable event $\{\mu_{t_0,\nu} > t\}$. Then,

$$\begin{aligned} \mathbb{E}[\|\omega_{t+1}\|^2 \mathbf{1}_{\mu_{t+1}} | \mathcal{F}_{t-1}] &\leq \mathbb{E}[\|\omega_{t+1}\|^2 \mathbf{1}_{\mu_t} | \mathcal{F}_{t-1}] \\ &\stackrel{(\text{C.7})}{\leq} \|\omega_t\|^2 \mathbf{1}_{\mu_t} + \beta_t^2 \|I - C_t\|^2 \|K_t^{-1}\|^2 \|\nabla\mathcal{L}_t\|^2 + \beta_t^2 \mathbb{E}[\|\theta_t\|^2 | \mathcal{F}_{t-1}] + \chi_t^2 \mathbb{E}[\|\mathbf{z}_{t,\tau}\|^2 | \mathcal{F}_{t-1}] \\ &\quad - 2\beta_t \langle (I - C_t)K_t^{-1}\nabla\mathcal{L}_t, \omega_t \mathbf{1}_{\mu_t} \rangle + 2\chi_t \|\omega_t\| \mathbf{1}_{\mu_t} \cdot \mathbb{E}[\|\mathbf{z}_{t,\tau}\| | \mathcal{F}_{t-1}] \\ &\quad + 2\beta_t \chi_t \|I - C_t\| \cdot \|K_t^{-1}\| \cdot \|\nabla\mathcal{L}_t\| \cdot \mathbb{E}[\|\mathbf{z}_{t,\tau}\| | \mathcal{F}_{t-1}] + 2\beta_t \chi_t \mathbb{E}[\|\theta_t\| \cdot \|\mathbf{z}_{t,\tau}\| | \mathcal{F}_{t-1}] \\ &\stackrel{(\text{C.1})}{\leq} \|\omega_t\|^2 \mathbf{1}_{\mu_t} + 4\Upsilon_K \Upsilon_u \beta_t^2 + C_{2+\delta}^{2/(2+\delta)} \beta_t^2 + \Upsilon_z \chi_t^2 - 2\beta_t \langle (I - C_t)K_t^{-1}\nabla\mathcal{L}_t, \omega_t \mathbf{1}_{\mu_t} \rangle + \frac{(1 - \rho^\tau)}{2} \beta_t \|\omega_t\|^2 \mathbf{1}_{\mu_t} \\ &\quad + \frac{2\Upsilon_z \chi_t^2}{(1 - \rho^\tau) \beta_t} + 4\Upsilon_K \Upsilon_u \sqrt{\Upsilon_z} \beta_t \chi_t + C_{2+\delta}^{2/(2+\delta)} \beta_t \chi_t + \Upsilon_z \beta_t \chi_t \\ &= (1 + 0.5(1 - \rho^\tau) \beta_t) \|\omega_t\|^2 \mathbf{1}_{\mu_t} - 2\beta_t \langle (I - C_t)K_t^{-1}\nabla\mathcal{L}_t, \omega_t \mathbf{1}_{\mu_t} \rangle + (4\Upsilon_K \Upsilon_u + C_{2+\delta}^{2/(2+\delta)}) \beta_t^2 + \Upsilon_z \chi_t^2 \\ &\quad + \frac{2\Upsilon_z \chi_t^2}{(1 - \rho^\tau) \beta_t} + (4\Upsilon_K \Upsilon_u \sqrt{\Upsilon_z} + C_{2+\delta}^{2/(2+\delta)} + \Upsilon_z) \beta_t \chi_t, \end{aligned} \quad (\text{C.8})$$

where the second inequality is also due to (11) and the fact that θ_t is the martingale difference; and the third inequality is also due to Lemma A.1(b), Lemma A.2(b), (C.2), and the fact $\|C_t\| \leq 1$. Since $\chi_t = c_\chi/(t+1)^\chi$, $\beta_t = c_\beta/(t+1)^\beta$ with $\chi > \beta + 0.5$ and $\beta \in (0.5, 1)$, we know

$$\chi_t^2 = o(\beta_t^2), \quad \frac{\chi_t^2}{\beta_t} = o(\beta_t^2), \quad \beta_t \chi_t = o(\beta_t^2).$$

For the second term on the right hand side of (C.8), we have for all $t_0 \leq t < \mu_{t_0,\nu}$,

$$\begin{aligned} -\langle (I - C_t)K_t^{-1}\nabla\mathcal{L}_t, \omega_t \rangle &= -\langle (I - C_t)\omega_t, \omega_t \rangle - \langle (I - C_t)(K_t^{-1}\nabla\mathcal{L}_t - \omega_t), \omega_t \rangle \\ &\leq -(1 - \rho^\tau) \|\omega_t\|^2 + 2\|K_t^{-1}\nabla\mathcal{L}_t - \omega_t\| \|\omega_t\| \quad (\text{Lemma A.1(c)}) \\ &\leq -(1 - \rho^\tau) \|\omega_t\|^2 + 2\Upsilon_K \|\nabla\mathcal{L}_t - K_t \omega_t\| \|\omega_t\| \quad (\text{Lemma A.2(b)}) \\ &\leq -(1 - \rho^\tau) \|\omega_t\|^2 + 2\Upsilon_K \nu \|\omega_t\|^2 + 2\Upsilon_K \|\nabla\mathcal{L}_t - K^* \omega_t\| \|\omega_t\| \quad (\text{by (C.5)}) \\ &\leq -(1 - \rho^\tau) \|\omega_t\|^2 + 2\Upsilon_K \nu \|\omega_t\|^2 + 2\Upsilon_K \Upsilon_L \|\omega_t\|^3 \quad (\text{by Assumption 3.1}) \\ &\leq -(1 - \rho^\tau) \|\omega_t\|^2 + 2\Upsilon_K (1 + \Upsilon_L) \nu \|\omega_t\|^2 \quad (\text{by (C.5)}) \\ &\leq -0.5(1 - \rho^\tau) \|\omega_t\|^2 \quad (\text{by (C.6)}). \end{aligned}$$

Combining the above two displays with (C.8), and applying Lemma A.4, we know there exists $\Upsilon_\mu^{(1)} > 0$ such that

$$\mathbb{E}[\|\omega_t\|^2 \mathbf{1}_{\{\mu_{t_0,\nu} > t\}}] \leq \Upsilon_\mu^{(1)} \beta_t, \quad \forall t \geq 0. \quad (\text{C.9})$$

Now, we establish the convergence rate of R_t . By the definition of R_t in (C.4), we have

$$\begin{aligned}
\mathbb{E}[R_t^2 \mathbf{1}_{\{\mu_{t_0, \nu} > t\}}] &\leq 2\mathbb{E} \left\| \frac{1}{t} \sum_{i=0}^{t-1} (\bar{H}_i - \nabla^2 f_i) \right\|^2 + \frac{2}{t^2} \mathbb{E} \left[\left(\sum_{i=0}^{t-1} \|\omega_i\| \right)^2 \mathbf{1}_{\{\mu_{t_0, \nu} > t\}} \right] \\
&\leq 2\mathbb{E} \left\| \frac{1}{t} \sum_{i=0}^{t-1} (\bar{H}_i - \nabla^2 f_i) \right\|^2 + \frac{2}{t^2} \mathbb{E} \left[\left(\sum_{i=0}^{t-1} \|\omega_i\| \mathbf{1}_{\{\mu_{t_0, \nu} > i\}} \right)^2 \right] \\
&\leq 2\mathbb{E} \left\| \frac{1}{t} \sum_{i=0}^{t-1} (\bar{H}_i - \nabla^2 f_i) \right\|^2 + \frac{2}{t^2} \left(\sum_{i=0}^{t-1} \mathbb{E}[\|\omega_i\|^2 \mathbf{1}_{\{\mu_{t_0, \nu} > i\}}]^{1/2} \right)^2, \quad (\text{C.10})
\end{aligned}$$

where the last inequality is from the Cauchy-Schwarz inequality. For the first term on the right hand side,

$$\begin{aligned}
\mathbb{E} \left\| \frac{1}{t} \sum_{i=0}^{t-1} (\bar{H}_i - \nabla^2 f_i) \right\|^2 &\leq \mathbb{E} \left\| \frac{1}{t} \sum_{i=0}^{t-1} (\bar{H}_i - \nabla^2 f_i) \right\|_F^2 = \frac{1}{t^2} \text{Tr} \left(\mathbb{E} \left(\sum_{i=0}^{t-1} (\bar{H}_i - \nabla^2 f_i) \right)^2 \right) \\
&= \frac{1}{t^2} \text{Tr} \left(\sum_{i=0}^{t-1} \mathbb{E}[(\bar{H}_i - \nabla^2 f_i)^2] \right) = \frac{1}{t^2} \sum_{i=0}^{t-1} \text{Tr}(\mathbb{E}[\mathbb{E}[\bar{H}_i^2 | \mathcal{F}_{i-1}] - (\nabla^2 f_i)^2]) \leq \frac{1}{t^2} \sum_{i=0}^{t-1} \mathbb{E}[\|\bar{H}_i\|_F^2] \leq \frac{d\Upsilon_m}{t},
\end{aligned}$$

where the third equality is because $\bar{H}_i - \nabla^2 f_i$ forms a martingale difference sequence with $\mathbb{E}[\bar{H}_i - \nabla^2 f_i | \mathcal{F}_{i-1}] = 0$, and the last inequality is due to Assumption 3.2. For the second term on the right hand side of (C.10), we apply (C.9) and have

$$\begin{aligned}
\frac{1}{t^2} \left(\sum_{i=0}^{t-1} \mathbb{E}[\|\omega_i\|^2 \mathbf{1}_{\{\mu_{t_0, \nu} > i\}}]^{1/2} \right)^2 &\leq \frac{\Upsilon_\mu^{(1)}}{t^2} \left(\sum_{i=0}^{t-1} \sqrt{\beta_i} \right)^2 = \frac{\Upsilon_\mu^{(1)} c_\beta}{t^2} \left(\sum_{i=0}^{t-1} \frac{1}{(i+1)^{0.5\beta}} \right)^2 \\
&\leq \frac{\Upsilon_\mu^{(1)} c_\beta}{t^2} \left(\int_0^t \frac{1}{(i+1)^{0.5\beta}} di \right)^2 \leq \frac{\Upsilon_\mu^{(1)} c_\beta}{(t+1)^\beta} = \Upsilon_\mu^{(1)} \beta_t.
\end{aligned}$$

Combining the above two displays and plugging into (C.10), we complete the proof.

D Additional Experimental Results

In this section, we present the complete experimental results in Tables 3-8 for constrained linear and logistic regression problems. We vary the dimension $d \in \{5, 20, 40\}$ and study three different design covariances Σ_a : Identity, Toeplitz, and Equi-correlation. Following prior work in [Chen et al. \(2020\)](#); [Na and Mahoney \(2025\)](#), we vary the parameter $r \in \{0.4, 0.5, 0.6\}$ for Toeplitz Σ_a and $r \in \{0.1, 0.2, 0.3\}$ for Equi-correlation Σ_a . We also vary the sketching steps of AI-SSQP $\tau \in \{20, 40, \infty\}$, where $\tau = \infty$ corresponds to the exact SSQP scheme. For each combination of d , Σ_a , and τ , we compare five different online inference procedures across four evaluation metrics: mean absolute error, averaged coverage rate, averaged confidence interval length, and flops per iteration.

We observe from Tables 3-8 that for both linear and logistic regression, the exact SSQP method ($\tau = \infty$) achieves a smaller mean absolute error than the inexact methods with $\tau = 20$ or 40 , between which $\tau = 40$ yields a smaller error than $\tau = 20$. In other words, the more accurate the Newton direction employed, the closer the method converges to the optimal solution. For the same setup of the

method, the inference procedures based on the averaged iterate (**AvePlugIn**, **AveBM**, **AveRS**) consistently yield the same mean absolute error, which is generally smaller, by half to one order of magnitude, than those based on the last iterate (**LastPlugIn**, **LastBF**). We notice that in some linear regression scenarios, the inexact methods result in abnormally high errors (e.g., $d = 5$, $\tau \in \{20, 40\}$, and Σ_a is identity or Equi-correlation with $r = 0.1$). This phenomenon is attributed to excessive randomness in approximating the Newton direction. A closer inspection reveals that in approximately 5 out of 200 runs, the inexact methods fail to converge; for the runs that do converge, the errors remain within a reasonable range. Moreover, when $d = 40$ and Σ_a is Equi-correlation with $r = 0.3$, the error for $\tau = 20$ is significantly higher than that for $\tau = 40$, likely due to insufficient accuracy in the Newton direction approximation. Overall, as suggested by the theory (cf. Remark 2.1), setting $\tau \gtrsim d$ appears to be a reasonable strategy for inexact methods to balance the trade-off between randomness and precision in the Newton direction approximation.

For the averaged coverage rate, we observe from Tables 3–8 that for a fixed dimension d , design covariance type Σ_a , and sketching step τ , all five inference methods exhibit certain robustness to variations in the parameter r . Among them, **AveRS** consistently achieves the nominal 95% coverage rate in most scenarios. **LastBF** performs comparably in terms of coverage but suffers from larger mean absolute errors and wider confidence intervals. The inference methods based on the plug-in covariance estimator, **LastPlugIn** and **AvePlugIn**, perform reasonably well when $\tau = \infty$ across different scenarios, with **AvePlugIn** yielding shorter confidence intervals. However, both methods tend to fail for maintaining the nominal 95% coverage rate when $\tau = 20, 40$ for both linear and logistic regression. There are exceptions: for instance, in linear regression with $d = 5$, **AvePlugIn** achieves coverage close to 95% across all design covariances, while **LastPlugIn** exhibits extreme overcoverage, approaching 100%. Conversely, in logistic regression with $d = 40$, **LastPlugIn** achieves near-nominal coverage across all designs, while **AvePlugIn** exhibits extreme undercoverage, falling below 80%. Overall, these failure modes stem from the inconsistency of the plug-in covariance estimator, rendering these methods *asymptotically invalid*. Lastly, we note that **AveBM** performs the worst among the five methods, with coverage rates far below acceptable levels. The batch-means estimator was originally designed for first-order methods with strongly convex objectives and/or sub-Gaussian gradient noise (Zhu et al., 2021; Jiang et al., 2025), and its theoretical guarantees do not extend to our setting.

In terms of the length of the confidence interval, we note that for each setup and inference method, the interval for logistic regression is consistently shorter than that for linear regression. Furthermore, **AveBM** and **AvePlugIn** yield the shortest intervals, reflecting the optimal efficiency of the averaged iterate due to its asymptotic normality guarantee, with **AveRS** performing nearly as well. In contrast, **LastBF** and **LastPlugIn** yield significantly wider intervals – roughly an order of magnitude larger – because the relative efficiency between the last and averaged iterates diverges under the stepsize schedule $\beta_t = 1/t^{0.501}$. This phenomenon demonstrates that our random scaling inference method retains much of the efficiency exhibited by covariance-estimation-based methods.

Finally, in terms of flops per iteration, it is clear that the inexact methods are matrix-free and incur lower computational costs compared to exact methods. The computational savings from the sketching solver become increasingly significant in higher dimensions. For example, in both linear and logistic regression with $d = 40$, **AveRS** with $\tau = 20$ achieves a 95% coverage rate across different design covariances with fewer than 1700 flops per iteration, while the exact method requires over 10^5 flops per iteration to achieve a similar coverage rate. This online, matrix-free fashion makes our inference method especially attractive for large-scale constrained problems.

d	Design Cov	Method	Constrained linear regression			Constrained logistic regression			Flops/iter	
			MAE (10^{-2})	Ave Cov (%)	Ave Len (10^{-2})	MAE (10^{-2})	Ave Cov (%)	Ave Len (10^{-2})		
5	Identity	$\tau = \infty$	LastPlugIn	9.14	94.00	7.81	3.21	93.50	1.37	487.60
			AvePlugIn	1.63	95.00	1.40	0.58	90.50	0.25	
			LastBF	9.14	94.00	7.70	3.21	95.00	1.46	365.40
			AveBM	1.63	67.00	0.74	0.58	60.50	0.15	
			AveRS		98.50	2.31		95.00	0.47	
		$\tau = 40$	LastPlugIn	63.90	98.00	9.65	2.85	90.00	1.37	424.60
			AvePlugIn	68.88	92.50	1.73	0.63	87.00	0.25	
			LastBF	63.90	91.50	4.83	2.85	93.50	1.48	302.40
			AveBM	68.88	56.00	1.19	0.63	62.50	0.16	
			AveRS		93.00	3.75		96.00	0.49	
		$\tau = 20$	LastPlugIn	46.20	98.50	10.08	2.76	89.00	1.38	284.60
			AvePlugIn	45.03	93.50	1.80	0.69	87.00	0.25	
			LastBF	46.20	88.00	3.22	2.76	91.00	1.50	162.40
			AveBM	45.03	35.50	0.83	0.69	65.00	0.16	
			AveRS		93.00	4.52		97.50	0.51	
	Toeplitz $r = 0.4$	$\tau = \infty$	LastPlugIn	7.25	96.00	6.44	2.92	89.00	1.48	487.60
			AvePlugIn	1.26	96.00	1.15	0.55	89.50	0.26	
			LastBF	7.25	96.00	6.32	2.92	92.50	1.62	365.40
			AveBM	1.26	71.50	0.58	0.55	66.50	0.17	
			AveRS		99.50	1.84		98.00	0.54	
		$\tau = 40$	LastPlugIn	4.38	100.00	6.45	2.62	90.50	1.47	424.60
			AvePlugIn	1.31	95.50	1.15	0.58	90.50	0.26	
			LastBF	4.38	91.50	3.41	2.62	93.00	1.57	302.40
			AveBM	1.31	57.00	0.48	0.58	68.00	0.17	
			AveRS		95.50	1.51		98.50	0.54	
		$\tau = 20$	LastPlugIn	3.86	100.00	6.46	2.48	94.00	1.48	284.60
			AvePlugIn	1.35	96.50	1.15	0.57	85.50	0.26	
			LastBF	3.86	95.00	2.89	2.48	96.00	1.58	162.40
			AveBM	1.35	53.50	0.42	0.57	65.50	0.17	
			AveRS		91.50	1.31		97.00	0.54	
	Toeplitz $r = 0.5$	$\tau = \infty$	LastPlugIn	7.81	98.00	6.53	2.93	88.50	1.48	487.60
			AvePlugIn	1.29	94.50	1.17	0.53	89.50	0.26	
			LastBF	7.81	97.50	6.47	2.93	89.50	1.60	365.40
			AveBM	1.29	65.00	0.59	0.53	67.00	0.17	
			AveRS		96.50	1.85		97.50	0.53	
		$\tau = 40$	LastPlugIn	4.45	100.00	6.54	2.55	94.50	1.48	424.60
			AvePlugIn	1.46	95.00	1.17	0.55	91.50	0.26	
			LastBF	4.45	95.50	3.40	2.55	96.00	1.61	302.40
			AveBM	1.46	51.00	0.49	0.55	70.00	0.17	
			AveRS		93.50	1.55		97.00	0.52	
		$\tau = 20$	LastPlugIn	9.57	99.50	6.73	2.45	93.00	1.48	284.60
			AvePlugIn	9.30	97.00	1.20	0.56	91.00	0.26	
			LastBF	9.57	93.00	4.03	2.45	94.00	1.56	162.40
			AveBM	9.30	53.50	0.92	0.56	64.50	0.16	
			AveRS		93.00	2.88		98.00	0.52	
	Toeplitz $r = 0.6$	$\tau = \infty$	LastPlugIn	7.93	93.50	6.63	2.89	90.50	1.48	487.60
			AvePlugIn	1.39	97.50	1.18	0.54	90.00	0.27	
			LastBF	7.93	92.00	6.50	2.89	91.50	1.61	365.40
			AveBM	1.39	64.50	0.61	0.54	70.00	0.17	
			AveRS		96.50	1.93		97.00	0.54	
		$\tau = 40$	LastPlugIn	4.31	100.00	6.63	2.54	92.00	1.48	424.60
			AvePlugIn	1.34	96.50	1.19	0.54	85.50	0.26	
			LastBF	4.31	95.00	3.39	2.54	95.50	1.60	302.40
			AveBM	1.34	56.50	0.50	0.54	59.50	0.16	
			AveRS		93.00	1.57		97.00	0.50	
		$\tau = 20$	LastPlugIn	3.92	100.00	6.62	2.34	95.50	1.48	284.60
			AvePlugIn	1.44	95.50	1.18	0.55	87.00	0.27	
			LastBF	3.92	94.00	2.94	2.34	96.00	1.57	162.40
			AveBM	1.44	51.50	0.43	0.55	63.50	0.17	
			AveRS		93.00	1.34		95.50	0.53	

Table 3: Comparison results for different inference methods on constrained linear and logistic regression problems under $d = 5$.

d	Design Cov	Method	Constrained linear regression			Constrained logistic regression			Flops/iter	
			MAE (10^{-2})	Ave Cov (%)	Ave Len (10^{-2})	MAE (10^{-2})	Ave Cov (%)	Ave Len (10^{-2})		
5	Equi-Corr $r = 0.1$	$\tau = \infty$	LastPlugIn	8.15	94.50	7.38	3.12	94.00	1.44	487.60
			AvePlugIn	1.41	97.00	1.32	0.59	92.00	0.26	
			LastBF	8.15	94.50	7.29	3.12	96.50	1.55	365.40
			AveBM	1.41	68.50	0.71	0.59	74.00	0.16	
			AveRS		99.00	2.23		96.50	0.49	
		$\tau = 40$	LastPlugIn	22.58	99.50	8.42	2.68	92.50	1.44	424.60
			AvePlugIn	20.16	93.50	1.51	0.62	90.50	0.26	
			LastBF	22.58	89.50	3.50	2.68	93.00	1.55	302.40
			AveBM	20.16	56.50	0.71	0.62	67.50	0.17	
		$\tau = 20$	AveRS		91.50	2.24		96.00	0.52	284.60
			LastPlugIn	71.46	99.00	11.27	2.61	90.00	1.44	
			AvePlugIn	69.78	93.00	2.01	0.65	89.00	0.26	
			LastBF	71.46	89.50	3.17	2.61	92.00	1.55	162.40
			AveBM	69.78	46.00	0.69	0.65	64.00	0.17	
			AveRS		88.50	2.17		97.50	0.55	
5	Equi-Corr $r = 0.2$	$\tau = \infty$	LastPlugIn	8.40	97.00	7.36	3.00	95.00	1.44	487.60
			AvePlugIn	1.50	95.50	1.32	0.59	90.00	0.26	
			LastBF	8.40	96.00	7.25	3.00	95.50	1.56	365.40
			AveBM	1.50	63.50	0.69	0.59	62.50	0.16	
			AveRS		97.50	2.17		95.00	0.50	
		$\tau = 40$	LastPlugIn	4.59	100.00	7.37	2.67	91.00	1.44	424.60
			AvePlugIn	1.52	96.00	1.32	0.63	86.00	0.26	
			LastBF	4.59	93.50	3.25	2.67	92.50	1.54	302.40
			AveBM	1.52	56.00	0.58	0.63	62.00	0.17	
		$\tau = 20$	AveRS		93.50	1.81		97.50	0.52	284.60
			LastPlugIn	4.17	100.00	7.37	2.53	93.00	1.44	
			AvePlugIn	1.48	95.00	1.32	0.62	87.50	0.26	
			LastBF	4.17	93.50	2.65	2.53	96.50	1.55	162.40
			AveBM	1.48	50.00	0.47	0.62	62.50	0.17	
			AveRS		87.00	1.46		95.50	0.52	
5	Equi-Corr $r = 0.3$	$\tau = \infty$	LastPlugIn	8.00	95.00	7.35	3.20	94.50	1.45	487.60
			AvePlugIn	1.49	96.00	1.31	0.61	86.00	0.26	
			LastBF	8.00	93.50	7.23	3.20	96.50	1.56	365.40
			AveBM	1.49	65.00	0.65	0.61	67.00	0.17	
			AveRS		98.00	2.05		98.00	0.53	
		$\tau = 40$	LastPlugIn	35.46	99.50	9.71	2.64	89.50	1.45	424.60
			AvePlugIn	32.76	92.50	1.74	0.61	87.50	0.26	
			LastBF	35.46	94.50	3.30	2.64	90.50	1.56	302.40
			AveBM	32.76	52.00	0.60	0.61	63.00	0.17	
		$\tau = 20$	AveRS		93.50	1.88		97.50	0.53	284.60
			LastPlugIn	3.94	100.00	7.36	2.58	92.50	1.45	
			AvePlugIn	1.47	95.50	1.32	0.62	92.00	0.26	
			LastBF	3.94	92.00	2.64	2.58	93.50	1.53	162.40
			AveBM	1.47	46.50	0.43	0.62	64.50	0.16	
			AveRS		87.00	1.35		97.00	0.50	

Table 4: (Cont') Comparison results for different inference methods on constrained linear and logistic regression problems under $d = 5$.

d	Design Cov	Method	Constrained linear regression			Constrained logistic regression			Flops/iter	
			MAE (10^{-2})	Ave Cov (%)	Ave Len (10^{-2})	MAE (10^{-2})	Ave Cov (%)	Ave Len (10^{-2})		
20	Identity	$\tau = \infty$	LastPlugIn	9.19	94.50	1.06	4.39	91.00	0.43	17632.74
			AvePlugIn	1.63	94.50	0.19	0.84	88.00	0.08	
			LastBF	9.19	94.50	1.05	4.39	93.50	0.46	14063.88
			AveBM	1.63	60.00	0.09	0.84	59.00	0.05	
			AveRS		97.50	0.29		95.00	0.14	
		$\tau = 40$	LastPlugIn	7.30	91.00	1.07	4.19	91.00	0.43	4768.87
			AvePlugIn	2.03	93.50	0.19	0.95	81.00	0.08	
			LastBF	7.30	92.50	1.09	4.19	95.00	0.47	1200.00
			AveBM	2.03	65.00	0.11	0.95	66.00	0.05	
			AveRS		96.00	0.36		95.50	0.17	
		$\tau = 20$	LastPlugIn	19.70	92.00	1.11	4.05	89.00	0.43	4288.87
			AvePlugIn	16.11	80.50	0.20	1.14	71.00	0.08	
			LastBF	19.70	94.50	1.14	4.05	94.00	0.50	720.01
			AveBM	16.11	57.50	0.13	1.14	59.00	0.06	
			AveRS		94.00	0.41		96.50	0.19	
	Toeplitz $r = 0.4$	$\tau = \infty$	LastPlugIn	9.02	96.50	1.44	4.25	90.50	0.47	17632.74
			AvePlugIn	1.65	93.00	0.26	0.82	92.00	0.08	
			LastBF	9.02	96.00	1.43	4.25	93.50	0.50	14063.88
			AveBM	1.65	63.00	0.13	0.82	63.50	0.05	
			AveRS		99.50	0.41		97.00	0.16	
		$\tau = 40$	LastPlugIn	44.63	97.50	1.71	4.05	94.00	0.47	4768.87
			AvePlugIn	39.68	91.00	0.31	0.94	88.00	0.08	
			LastBF	44.63	92.50	1.30	4.05	95.00	0.52	1200.00
			AveBM	39.68	58.50	0.21	0.94	68.50	0.06	
			AveRS		93.50	0.65		96.50	0.17	
		$\tau = 20$	LastPlugIn	27.28	97.50	1.59	3.90	86.50	0.47	4288.87
			AvePlugIn	22.66	86.50	0.28	1.11	72.50	0.08	
			LastBF	27.28	93.50	1.18	3.90	91.50	0.53	720.01
			AveBM	22.66	57.50	0.14	1.11	53.50	0.06	
			AveRS		92.50	0.45		94.50	0.20	
	Toeplitz $r = 0.5$	$\tau = \infty$	LastPlugIn	8.99	96.50	1.46	4.16	91.50	0.47	17632.74
			AvePlugIn	1.67	93.50	0.26	0.78	93.50	0.08	
			LastBF	8.99	96.50	1.45	4.16	93.00	0.50	14063.88
			AveBM	1.67	63.00	0.13	0.78	58.50	0.05	
			AveRS		95.50	0.42		98.00	0.15	
		$\tau = 40$	LastPlugIn	7.31	99.00	1.46	4.01	92.00	0.47	4768.87
			AvePlugIn	2.03	93.00	0.26	0.92	86.50	0.08	
			LastBF	7.31	96.00	1.12	4.01	95.50	0.53	1200.00
			AveBM	2.03	56.00	0.12	0.92	66.00	0.06	
			AveRS		94.50	0.39		98.00	0.19	
		$\tau = 20$	LastPlugIn	7.12	98.50	1.46	3.85	92.50	0.48	4288.87
			AvePlugIn	2.34	88.00	0.26	1.08	75.00	0.08	
			LastBF	7.12	93.00	1.15	3.85	94.50	0.53	720.01
			AveBM	2.34	54.00	0.13	1.08	60.00	0.07	
			AveRS		91.50	0.42		98.00	0.21	
	Toeplitz $r = 0.6$	$\tau = \infty$	LastPlugIn	8.76	96.50	1.49	4.16	91.00	0.48	17632.74
			AvePlugIn	1.66	95.00	0.27	0.76	93.00	0.09	
			LastBF	8.76	96.00	1.46	4.16	94.00	0.50	14063.88
			AveBM	1.66	68.00	0.14	0.76	71.00	0.05	
			AveRS		98.50	0.43		97.00	0.16	
		$\tau = 40$	LastPlugIn	7.24	98.00	1.32	3.95	88.00	0.48	4768.87
			AvePlugIn	1.94	92.50	0.24	0.89	82.50	0.09	
			LastBF	7.24	95.50	1.15	3.95	91.00	0.52	1200.00
			AveBM	1.94	67.50	0.13	0.89	56.50	0.05	
			AveRS		94.50	0.39		97.00	0.17	
		$\tau = 20$	LastPlugIn	7.00	99.50	1.49	3.75	90.50	0.48	4288.87
			AvePlugIn	2.40	87.00	0.27	1.05	85.50	0.09	
			LastBF	7.00	96.50	1.16	3.75	92.50	0.54	720.01
			AveBM	2.40	54.00	0.13	1.05	66.50	0.07	
			AveRS		93.50	0.40		97.50	0.22	

Table 5: Comparison results for different inference methods on constrained linear and logistic regression problems under $d = 20$.

d	Design Cov	Method	Constrained linear regression			Constrained logistic regression			Flops/iter	
			MAE (10^{-2})	Ave Cov (%)	Ave Len (10^{-2})	MAE (10^{-2})	Ave Cov (%)	Ave Len (10^{-2})		
20	Equi-Corr $r = 0.1$	$\tau = \infty$	LastPlugIn	8.84	94.00	1.38	4.17	94.50	0.44	17632.74
			AvePlugIn	1.61	94.00	0.25	0.80	94.00	0.08	
			LastBF	8.84	93.50	1.37	4.17	94.50	0.46	
			AveBM	1.61	63.00	0.13	0.80	64.00	0.04	14063.88
			AveRS		97.00	0.40		98.50	0.14	
		$\tau = 40$	LastPlugIn	7.26	97.00	1.38	3.98	90.00	0.44	4768.87
			AvePlugIn	1.87	91.00	0.25	0.92	83.50	0.08	
			LastBF	7.26	94.50	1.16	3.98	92.00	0.47	
			AveBM	1.87	58.50	0.13	0.92	60.00	0.05	1200.00
		$\tau = 20$	AveRS		95.00	0.41		95.00	0.17	
			LastPlugIn	7.34	95.50	1.38	3.79	88.00	0.43	4288.87
			AvePlugIn	2.19	88.50	0.25	1.08	78.50	0.08	
			LastBF	7.34	93.50	1.21	3.79	93.00	0.48	
			AveBM	2.19	55.00	0.15	1.08	94.50	0.06	720.01
			AveRS		94.00	0.46		94.50	0.18	
20	Equi-Corr $r = 0.2$	$\tau = \infty$	LastPlugIn	8.92	95.00	1.40	4.07	94.50	0.43	17632.74
			AvePlugIn	1.59	96.00	0.25	0.76	92.50	0.08	
			LastBF	8.92	94.00	1.36	4.07	94.00	0.45	
			AveBM	1.59	60.50	0.12	0.76	64.00	0.04	14063.88
			AveRS		98.00	0.39		97.50	0.14	
		$\tau = 40$	LastPlugIn	7.43	99.50	1.40	3.81	94.00	0.42	4768.87
			AvePlugIn	1.93	89.50	0.25	0.87	92.00	0.08	
			LastBF	7.43	94.50	1.15	3.81	95.00	0.46	
			AveBM	1.93	57.00	0.13	0.87	70.00	0.05	1200.00
			AveRS		94.50	0.39		98.50	0.16	
		$\tau = 20$	LastPlugIn	57.67	95.00	1.82	3.70	90.50	0.43	4288.87
			AvePlugIn	54.55	86.50	0.32	1.08	77.50	0.08	
			LastBF	57.67	93.00	1.41	3.70	95.00	0.47	
			AveBM	54.55	52.50	0.24	1.08	60.00	0.06	720.01
			AveRS		94.00	0.75		95.50	0.18	
20	Equi-Corr $r = 0.3$	$\tau = \infty$	LastPlugIn	8.96	95.00	1.41	3.92	92.00	0.41	17632.74
			AvePlugIn	1.62	96.00	0.25	0.73	94.00	0.07	
			LastBF	8.96	95.50	1.38	3.92	93.00	0.43	
			AveBM	1.62	63.50	0.13	0.73	64.50	0.04	14063.88
			AveRS		97.00	0.39		98.50	0.14	
		$\tau = 40$	LastPlugIn	25.10	96.50	1.63	3.79	89.50	0.41	4768.87
			AvePlugIn	20.68	87.00	0.29	0.85	81.50	0.07	
			LastBF	25.10	93.50	1.26	3.79	92.50	0.45	
			AveBM	20.68	52.00	0.19	0.85	58.50	0.05	1200.00
			AveRS		92.00	0.59		96.00	0.15	
		$\tau = 20$	LastPlugIn	30.27	97.50	1.67	3.57	89.00	0.41	4288.87
			AvePlugIn	25.89	87.00	0.30	1.02	79.50	0.07	
			LastBF	30.27	94.00	1.23	3.57	92.50	0.46	
			AveBM	25.89	55.50	0.15	1.02	65.00	0.06	720.01
			AveRS		89.50	0.48		95.50	0.19	

Table 6: (Cont') Comparison results for different inference methods on constrained linear and logistic regression problems under $d = 20$.

d	Design Cov	Method	Constrained linear regression			Constrained logistic regression			Flops/iter	
			MAE (10^{-2})	Ave Cov (%)	Ave Len (10^{-2})	MAE (10^{-2})	Ave Cov (%)	Ave Len (10^{-2})		
40	Identity	$\tau = \infty$	LastPlugIn	10.68	97.00	0.62	5.63	95.00	0.28	106068.43
			AvePlugIn	1.93	94.00	0.11	1.07	90.00	0.05	
			LastBF	10.68	95.50	0.61	5.63	95.50	0.29	85975.21
			AveBM	1.93	60.00	0.06	1.07	59.00	0.03	
			AveRS		96.00	0.18		96.00	0.09	
		$\tau = 40$	LastPlugIn	10.19	86.00	0.62	5.16	89.50	0.28	22645.27
			AvePlugIn	2.60	81.00	0.11	1.43	78.00	0.05	
			LastBF	10.19	93.50	0.76	5.16	91.50	0.30	2552.05
			AveBM	2.60	64.00	0.08	1.43	65.00	0.04	
			AveRS		97.00	0.26		96.50	0.13	
		$\tau = 20$	LastPlugIn	10.21	85.00	0.62	5.07	89.50	0.28	21765.28
			AvePlugIn	3.26	74.50	0.11	1.80	69.50	0.05	
			LastBF	10.21	92.50	0.78	5.07	90.50	0.30	1672.05
			AveBM	3.26	62.00	0.10	1.80	59.00	0.05	
			AveRS		94.00	0.32		95.50	0.14	
	Toeplitz $r = 0.4$	$\tau = \infty$	LastPlugIn	10.92	96.00	0.59	5.55	93.00	0.29	106068.43
			AvePlugIn	1.95	98.00	0.11	1.03	93.50	0.05	
			LastBF	10.92	94.50	0.58	5.55	93.00	0.30	85975.21
			AveBM	1.95	62.50	0.05	1.03	64.50	0.03	
			AveRS		96.00	0.16		98.00	0.09	
		$\tau = 40$	LastPlugIn	10.27	87.50	0.59	4.89	91.00	0.29	22645.27
			AvePlugIn	2.65	79.00	0.11	1.38	81.00	0.05	
			LastBF	10.27	93.50	0.77	4.89	92.50	0.30	2552.05
			AveBM	2.65	65.00	0.08	1.38	65.00	0.04	
			AveRS		97.50	0.25		97.00	0.12	
		$\tau = 20$	LastPlugIn	10.11	84.50	0.59	4.80	91.50	0.29	21765.28
			AvePlugIn	3.31	74.00	0.11	1.71	65.00	0.05	
			LastBF	10.11	94.50	0.78	4.80	89.00	0.29	1672.05
			AveBM	3.31	67.50	0.10	1.71	59.00	0.05	
			AveRS		96.00	0.30		93.00	0.15	
	Toeplitz $r = 0.5$	$\tau = \infty$	LastPlugIn	10.73	94.00	0.59	5.28	94.00	0.30	106068.43
			AvePlugIn	1.96	95.50	0.11	0.99	90.50	0.05	
			LastBF	10.73	94.00	0.58	5.28	94.00	0.31	85975.21
			AveBM	1.96	66.50	0.06	0.99	68.00	0.03	
			AveRS		94.50	0.18		96.00	0.10	
		$\tau = 40$	LastPlugIn	10.15	84.50	0.59	4.84	95.00	0.30	22645.27
			AvePlugIn	2.67	80.50	0.10	1.38	79.00	0.05	
			LastBF	10.15	95.50	0.77	4.84	92.50	0.30	2552.05
			AveBM	2.67	60.50	0.07	1.38	62.00	0.04	
			AveRS		97.00	0.23		95.50	0.12	
		$\tau = 20$	LastPlugIn	9.94	82.50	0.59	4.63	92.00	0.30	21765.28
			AvePlugIn	3.31	77.50	0.10	1.68	71.50	0.05	
			LastBF	9.94	94.00	0.79	4.63	94.50	0.30	1672.05
			AveBM	3.31	65.00	0.09	1.68	58.50	0.05	
			AveRS		96.50	0.30		95.00	0.15	
	Toeplitz $r = 0.6$	$\tau = \infty$	LastPlugIn	10.80	94.50	0.58	5.19	94.50	0.30	106068.43
			AvePlugIn	1.97	95.00	0.10	0.97	90.00	0.05	
			LastBF	10.80	95.00	0.57	5.19	96.00	0.31	85975.21
			AveBM	1.97	67.00	0.05	0.97	61.00	0.03	
			AveRS		97.50	0.16		96.50	0.09	
		$\tau = 40$	LastPlugIn	10.22	88.50	0.58	4.68	94.00	0.30	22645.27
			AvePlugIn	2.74	85.00	0.10	1.34	82.00	0.05	
			LastBF	10.22	97.00	0.78	4.68	93.50	0.30	2552.05
			AveBM	2.74	67.00	0.08	1.34	60.50	0.04	
			AveRS		95.50	0.25		96.00	0.12	
		$\tau = 20$	LastPlugIn	10.17	87.50	0.58	4.52	92.50	0.30	21765.28
			AvePlugIn	3.40	75.00	0.10	1.65	70.50	0.05	
			LastBF	10.17	97.00	0.80	4.52	89.50	0.29	1672.05
			AveBM	3.40	69.00	0.09	1.65	53.50	0.05	
			AveRS		96.00	0.28		93.50	0.14	

Table 7: Comparison results for different inference methods on constrained linear and logistic regression problems under $d = 40$.

d	Design Cov	Method	Constrained linear regression			Constrained logistic regression			Flops/iter	
			MAE (10^{-2})	Ave Cov (%)	Ave Len (10^{-2})	MAE (10^{-2})	Ave Cov (%)	Ave Len (10^{-2})		
40	Equi-Corr $r = 0.1$	$\tau = \infty$	LastPlugIn	10.83	94.50	0.67	5.29	94.50	0.28	106068.43
			AvePlugIn	1.95	95.50	0.12	0.98	91.00	0.05	
			LastBF	10.83	94.50	0.65	5.29	97.00	0.29	
			AveBM	1.95	63.50	0.06	0.98	68.50	0.03	85975.21
			AveRS		97.50	0.20		97.50	0.09	
		$\tau = 40$	LastPlugIn	10.16	87.50	0.67	4.91	91.50	0.28	22645.27
			AvePlugIn	2.65	90.00	0.12	1.31	80.00	0.05	
			LastBF	10.16	93.50	0.81	4.91	92.50	0.29	
			AveBM	2.65	65.50	0.08	1.31	65.00	0.04	2552.05
			AveRS		96.00	0.26		96.00	0.12	
		$\tau = 20$	LastPlugIn	10.19	89.00	0.67	4.67	90.50	0.28	21765.28
			AvePlugIn	3.37	75.50	0.12	1.65	66.00	0.05	
			LastBF	10.19	96.00	0.85	4.67	92.00	0.29	
			AveBM	3.37	59.00	0.10	1.65	55.50	0.04	1672.05
			AveRS		96.50	0.30		96.50	0.13	
	Equi-Corr $r = 0.2$	$\tau = \infty$	LastPlugIn	10.95	94.50	0.66	4.85	95.00	0.27	106068.43
			AvePlugIn	1.97	95.50	0.12	0.90	92.50	0.05	
			LastBF	10.95	94.50	0.65	4.85	95.00	0.28	
			AveBM	1.97	70.00	0.06	0.90	69.00	0.03	85975.21
			AveRS		99.00	0.19		97.00	0.09	
		$\tau = 40$	LastPlugIn	10.31	92.00	0.66	4.52	94.50	0.27	22645.27
			AvePlugIn	2.83	86.00	0.12	1.21	80.50	0.05	
			LastBF	10.31	94.50	0.78	4.52	94.50	0.27	
			AveBM	2.83	65.00	0.08	1.21	63.50	0.03	2552.05
			AveRS		96.50	0.25		96.50	0.11	
		$\tau = 20$	LastPlugIn	10.16	89.00	0.66	4.41	94.50	0.27	21765.28
			AvePlugIn	3.46	78.50	0.12	1.52	69.00	0.05	
			LastBF	10.16	96.00	0.84	4.41	94.00	0.28	
			AveBM	3.46	60.00	0.09	1.52	61.00	0.04	1672.05
			AveRS		94.50	0.28		94.50	0.13	
	Equi-Corr $r = 0.3$	$\tau = \infty$	LastPlugIn	11.21	95.00	0.65	4.68	92.50	0.26	106068.43
			AvePlugIn	2.05	93.00	0.12	0.85	92.50	0.05	
			LastBF	11.21	93.50	0.65	4.68	93.00	0.26	
			AveBM	2.05	64.50	0.06	0.85	67.50	0.03	85975.21
			AveRS		97.00	0.18		96.50	0.08	
		$\tau = 40$	LastPlugIn	10.11	90.00	0.65	4.27	96.50	0.26	22645.27
			AvePlugIn	2.91	88.00	0.12	1.13	83.50	0.05	
			LastBF	10.11	95.00	0.75	4.27	96.50	0.26	
			AveBM	2.91	62.50	0.08	1.13	64.50	0.03	2552.05
			AveRS		95.00	0.24		98.00	0.10	
		$\tau = 20$	LastPlugIn	35.73	84.50	0.82	4.10	95.00	0.26	21765.28
			AvePlugIn	30.53	80.00	0.15	1.41	71.00	0.05	
			LastBF	35.73	90.50	0.91	4.10	93.00	0.26	
			AveBM	30.53	59.50	0.13	1.41	60.50	0.04	1672.05
			AveRS		95.50	0.41		98.00	0.11	

Table 8: (Cont') Comparison results for different inference methods on constrained linear and logistic regression problems under $d = 40$.